

Response to RC 1

To begin, the authors would like to thank the reviewer for their time, attention to detail, and insights on the paper and research. Each comment will be addressed point by point. The * next to line numbers indicates that it is referencing the tracked-changes manuscript. The * next to figure numbers references the supplemental figures in this response to the reviewer and not the original manuscript.

Specific Comments:

I.175: What is the meaning of 'coupled'? Probably only the use of the mineral dust emissions module (but not the transport, mixing, deposition etc.). Please better explain.

Here, the term “coupled” indicates that the meteorology (WRF) and the aerosol module (GOCART) are combined in the model in a way that they can directly impact each other. This is not just the meteorology and land surface part of the code being connected to dust emissions (e.g. wind speed, soil moisture, etc.), but also dust transportation via advection, convection, and turbulent mixing, as well as dry / wet deposition, and aerosol radiation effects. The rates for all of these dust processes are inextricably linked to the meteorology, and are treated such in the code via the direct coupling of WRF to the GOCART model. Additional clarification of “coupled” was added to this paragraph for readers:

Ln 154-156* [The model is coupled to the Goddard Chemistry Aerosol Radiation and Transport (GOCART) module (Ginoux et al., 2001), which allows for feedbacks between the meteorology and aerosols and is described in more detail in Sect. 2.2.]

Ln 184-186* [...it is then transported based on the simulated meteorological fields from WRF, including advection, convection, and turbulent mixing...]

I.177 More details are needed about the schemes used. The paper is a sensitivity study about these schemes and they are not explained. In particular, the way to treat the aerosol for the indirect effects is completely different (the Grell scheme is aerosol aware compared to the others).

There is a paragraph later in the manuscript that points out the major differences between the cumulus schemes tested (Ln 230-240*). The Grell aerosol-aware scheme mentioned by the reviewer is the Grell-Freitas Ensemble Scheme (Grell & Freitas, 2014), whereas the one tested here is the non-aerosol aware version referred to as the Grell 3D Ensemble Scheme (Grell 1993; Grell & Devenyi, 2002). The aerosol aware scheme was not tested because it depends on the modelled aerosol number concentration affecting the CCN number. However, the GOCART aerosol module is a single-moment in mass scheme, which means it carries no number information and cannot alter the CCN number. As such, the GOCART model wouldn't have an effect on the aerosol aware version.

The overarching point of this study is that resolution matters more than the choice of convective parameterization. Thus, the point of including several cumulus parameterization schemes rather than just one was to represent the uncertainty across a spread of different available options in the model, and not to attribute why one scheme produces one solution or another. That is why at no point in the paper are the cumulus parameterizations directly compared to each other. Rather, they are represented as an ensemble mean with uncertainty estimates. Comparing the detailed responses of individual

schemes to each other is outside the scope of this paper, but absolutely warrants further study and could be an entire manuscript on its own merit.

I.178: for a mineral dust study "no chemistry" why not. But no initial and boundary conditions for a simulation of 3 days, it is not possible to have realistic results

The only aerosol the authors were interested in for this study was dust. Furthermore, the aerosol burden over the deserts in the Arabian Peninsula is dominated by mineral dust (Heald et al. 2014), and as such, the authors decided that the full atmospheric chemistry code in WRF-Chem (e.g. gas phase and aqueous chemistry, etc.) was not needed and that other aerosol species were outside the scope of this study.

Two additional test cases were performed to address the reviewer's comment relating to the use of initial and lateral boundary conditions. First, a 3 km BMJ simulation was run using both initial conditions (ICs) and boundary conditions (BCs) for dust from the Community Atmosphere Model with Chemistry (CAM-Chem) global model, the output of which can be used for initializing the aerosol and chemistry fields in the mesoscale WRF-Chem model. Second, a 3 km BMJ simulation was run with only the lateral boundary conditions from CAM-Chem.

In the attached supplementary figures (denoted by a * to differentiate them from the figures in the manuscript), it can be seen that these two test cases (labeled as "BMJ-bcs and ics" and "BMJ-bcs only") have very little effect on the dust uplift potential (Fig. 4*), the threshold velocity, surface settling flux, bowen ratio (Fig. 5*), or the mean vertical velocity (Fig. 8A*). This is expected, since all of these fields are dominated by the meteorology and not the dust concentrations in the local environment.

Furthermore, the second test case "BMJ-bcs only," in which only lateral BCs were used to represent dusty air moving across the domain from places like the Sahara, has essentially no effect on the results and is in line with the conclusions from the manuscript where no lateral BCs were used. Including the BCs has minimal influence on integrated dust (Fig. 6A*), vertical dust concentrations (Fig. 7A*), dust fluxes (Fig. 8C*), or dust radiative effects (Fig. 11*). There are two possible interpretations of this result. One is that the dust concentrations being transported laterally into the domain are small for this case study. A second possibility is that the CAM-Chem model underestimates this dust source.

Conversely, including dust ICs ("BMJ-bcs and ics") does have an effect on the dust concentrations in the domain. Looking at the integrated dust plot (Fig. 6A*), there is a decreasing trend starting from the initial timestep throughout the rest of the simulation. The decreasing trend is not seen in the AOD observations from AERONET in the region (Fig. 12*). This points to the ICs being significantly higher than what the model produces on its own, and they are out of sync with the equilibrium model solution. Furthermore, comparing modeled AOD to the AERONET stations, there is little added benefit in using the ICs to get better agreement with observations. The model underpredicts dust throughout the simulation compared to observations, which is a finding in Saleeby et al. 2019, where this particular case study simulation is further compared to observations. It would most likely be better to adjust the dust tuning parameter (C) in Eq. 1 than to use ICs that are not in tune across modeling platforms or in keeping with the observations. The result of the added dust in the IC run is higher integrated dust (Fig. 6A*), vertical dust (Fig. 7A*), dust flux (Fig. 8C*), and a stronger radiative effect. While including dust ICs increases the dust load, it does not however change the conclusions of the study.

Saleeby, S. M., van den Heever, S. C., Bukowski, J., Walker, A. L., Solbrig, J. E., Atwood, S. A., Bian, Q., Kreidenweis, S. M., Wang, Y., Wang, J., and Miller, S. D.: The influence of simulated surface dust lofting and atmospheric loading on radiative forcing, *Atmos. Chem. Phys.*, 19, 10279–10301, <https://doi.org/10.5194/acp-19-10279-2019>, 2019.

I.182 "kept constant" meaning remain the same during the whole simulation?

Correct, and that these physics options don't change across the simulations – the language has been changed in the manuscript to remove any confusion:

Ln 162* [The following model parameterizations were employed and kept constant across the simulations..]

I.214: The 'Dust Uplift Potential' is a calculation already done in a large majority of dust emissions schemes, by principle of the mechanism to evaluate. Unfortunately, it represents only a small part of the problem and is not really useful. It describes only the link between the friction velocity threshold (using the aeolian roughness length) and the current friction velocity. But other important parameters are not taken into account: the vegetation, the erodibility, the soil humidity, the recent precipitation etc. In addition, the fact to use a constant U_t is not realistic (eq.3): the aeolian roughness length is far to be constant over erodible region. It is the most important varying parameter in mineral dust emissions modelling. The use of three different kind of DUP has a large interest. The message is already contained in one. If the authors really want to use this criteria, only one is enough.

The authors are not sure exactly as to what is being asked here by the reviewer. However, we have done our best to address the questions here as we understand them and hope this will address the reviewer's concern.

Several of the parameters listed here are contained in the varying DUP equations, including the erodibility (Eq. 5 with the variable S) and the soil moisture / recent precipitation (Eq. 4 and 5 depend on U_t - the only varying parameter in Eq. 2 for U_t is soil wetness, w_{soil}). The point of including these different DUP parameters is to tease out which of these processes is the most important without assuming that one is more important than the other for this case study. It has been shown previously in the literature that the soil moisture and erodibility are important for dust uplift (i.e. Gherboudj et al. 2015) in addition to wind speed, which means that using only one parameter doesn't tell the whole story.

Eq. 3, which is the most simplistic of the equations and assumes a constant roughness length, and has been used widely in the literature, especially in offline model dust approximations. To compare our results with that of other studies, it is necessary that we use Eq. 3. However, we point out its limitations and have included the more complicated DUP parameters we think are more useful for this study:

Ln 205-207* [This simplified equation for dust uplift has been used in previous dust studies, and is useful to include here to place the findings of this manuscript in the context of existing literature.]

I.239: The reference simulation has an horizontal resolution of 3km to enable explicit convection calculation. This simulation has boundary conditions and this is a good point. But these boundary conditions are from the BMJ simulation, i.e one of the studied case. Thus, we can think that the reference case will be very influenced by this case, no? To have a more realistic comparison between scheme, the

'reference' has to be done for each scheme and a first spread can be calculated between all 'high resolution' cases.

This is a good point – especially since there are two competing classes of cumulus parameterizations tested here: BMJ is the only moisture / temperature adjustment scheme, whereas the others are mass flux schemes. To test the sensitivity of the results to which cumulus parameterization scheme is employed in the parent nest, a second 3 km simulation was run. In this test, the Kain-Fritsch cumulus scheme serves as the 15 km parent, which is then nested to 3 km (this run is labeled as “3 km – KF” throughout the supplementary figures) to represent the mass-flux schemes. In none of the figures (Fig. 4-11*) is this difference significant or does it change the conclusions of this paper. Again, because model resolution dominates over the choice of cumulus parameterization, this effect of using a different parameterization in the outer nest has little effect on the results.

Ln 227-228* [Other combinations of nests were tested, but the results were not sensitive to which 15 km simulation was used as the parent nest, or which lateral boundary conditions, for the 3 km simulation.]

I.263: for long-range transport, 24h of spin-up is not enough. For the time averaged results, it is only the last two days. But for the time series, it is the 3 days? why this difference?

For the long-range transport part of this comment – see the response and tests from comment I.178. Including the lateral boundary conditions that represent long-range dust transport have little impact on the results and hence we feel that 24h of spin-up is sufficient.

For the time averaged results, we did not want to include the 24-hour model spin up time. However, they were included in the time series to show how the model approaches its equilibrium solution when starting from no dust sources.

I.272: why not use directly the mineral dust emissions fluxes? Please explain this important point.

The emission fluxes convey the same story as the approach utilized here (see Fig. 13*). However, the difference in the magnitude across the simulations is difficult to see in this plot, and it wasn't included. The conclusions are the same from a dust emission standpoint versus a dust concentration perspective. Additionally, the variables that go into the emission flux formula in GOCART (Eq. 1) are very similar to the Dust Uplift Potential (DUP) calculations. The most complete DUP parameter (Eq. 5) includes the same variables as the emission flux, so it would be redundant to include both the DUP calculations and the emission fluxes.

I.280: why the simulation with the coarsest resolution (and not simulation) overestimates the wind speed? Please explain (and I imagine it is the "10-m wind speed", please correct).

Correct – it is the 10-m wind speed. This has been updated in the manuscript:

Ln 297-298* [The coarsest simulation overestimates the near-surface wind speeds related to the NLLJ mechanism, which...]

There are a few theories regarding why the coarsest simulation would overestimate the near-surface wind speed. Marsham et al. (2011) noted that in their simulations over Northern Africa, the Saharan

Heat Low was more pronounced in the coarse simulations. They postulated that cold pool venting in the explicit simulations reduced this thermal low, thereby reducing the horizontal pressure gradients which are responsible for low-level jets in this region. It follows then that the low-level jet is weaker in this scenario, as is the process of mixing of the jet to the surface, and thus the near-surface wind speeds. In the Arabian Peninsula case study, this mechanism is certainly quite possible. However, this theory has yet to be tested and is outside the scope of this paper.

I.293: Yes, it is right. And obvious. Of course, a key point in modelling is to try to have a model not sensitive to the spatial resolution. And it seems it is the problem with WRF-chem. In WRF, the principle is to use, for each grid cell, the dominant soil type and landuse. Thus, by principle, the result is very sensitive to the resolution. Some other models are using subgrid scale variability and Weibull distribution for the 10-m wind speed, for example, to avoid this problem. Please see bibliography and replace WRF-chem in the context of all currently used regional dust models.

WRF-Chem is just one of many regional models that can be used operationally and / or in research applications. For instance, The Sand and Dust Storm Warning Advisory and Assessment System (SDS-WAS) includes 12 dust models, with more undoubtedly available to be used in research applications. Each model is unique, and most likely has several options for their cumulus parameterizations as well as other physical representations of meteorological processes. Combining the differences between dust models in this way is a very large undertaking the likes of which are being conducted by organized working groups like the International Cooperative for Aerosol Prediction (ICAP) and is outside the capabilities of a single manuscript.

I.331: it is not sure that there is an interest to have a conclusion such as "resolution increases or decreases the mineral dust emission fluxes". In fact it depends on the studied area, the variability of the orography, aeolian roughness length, soil humidity, vegetation. And, of course, the way to well take into account or not all these processes and their variability.

The reviewer makes an excellent point here. The manuscript has been updated to include more about the uncertainty here:

Ln 355-360* [...dust emissions and airborne dust mass increases in the WRF-Chem simulations in the convection-allowing simulation, which is in closer agreement to the studies of Reinfried et al. (2009) and Bouet et al. (2012) who used COSMO-MUSCAT and RAMS-DPM respectively. Considering each study used a different model and therefore physics, it is unsurprising that the results vary. However, it is not apparent how much of a role the region or specific case study plays in this difference and is an area for future work.]

I.335: I don't understand the discussion with "The rates of gravitational settling are higher in the explicit simulation compared to the coarse simulations, yet Fig. 6.a suggests that this is not enough to offset the higher dust emissions, or the integrated dust quantities would be similar across all the simulations." The dry deposition is proportional to the concentrations, being a velocity applied to the concentrations. How is it possible to have 'enough' settling to 'offset' the higher dust emissions?

If there is more dust aloft, more dust eventually needs to settle out. The point that we are trying to make here is that the missing piece in this process is the higher vertical transport. If dust was transported to the same height, the gravitational settling would offset the higher emissions and there

would be no reason for the integrated dust values to be higher. This part of the manuscript has been edited for clarity.

Ln 364-367* [The rates of gravitational settling are higher in the convection-permitting simulation compared to the coarse simulations because more dust is available aloft to settle out. Nevertheless, Fig. 6.a suggests that this increase in gravitational settling rates in the 3 km case is not enough to offset the higher dust emissions...]

Figure 6: the fact to have difference sbetween resolution is understandable but a factor 2 has to be better explained. Mineral dust emissions mass maps for the common domain (the one with 3km horizontal resolution). The caption is not easy to understand: "Domain averaged integrated dust mass". Please correct with Spatially averaged, vertically integrated.

The difference between resolutions in Figure 6 differ by a factor of 1.5, which we discuss in the previous section with Figure 4 and Figure 5. Using DUP(U,Ut,S) we see that the 3 km has the most potential to loft dust, especially on 04-Aug when there is a convective maximum. This is related to the threshold velocity being lower and soil wetness (Figure 5) and is also explained with the differences in vertical transport, which is covered in the next section of the manuscript. More about the differences in precipitation in convection-allowing versus parameterized simulations affecting soil moisture and the threshold velocity has been included in the text:

Ln 308-312* [Rainfall is generated differently in parameterized versus convection-allowing simulations, and it has been well documented that parameterized simulations produce more widespread light rainfall, whereas more intense rainfall tends to develop over smaller areas in convection-allowing simulations (e.g. Sun et al., 2006; Stephens et al., 2010). From a domain average perspective, rainfall in the 3 km simulation will cover less area, leading to the soil moisture threshold not being exceeded as frequently compared to the parameterized cases.]

These figures have been updated for clarity and the captions have been changed. Throughout the manuscript anytime there is a reference to "domain averaged integrated dust" it has been changed to the phrase "spatially averaged, vertically integrated."

Ln 911* [Figure 6: Spatially averaged, vertically integrated dust mass. Colors and shading are identical to that in previous figures.]

l.346: "the vertical dust profile follows a generally exponentially decreasing function" is it a conclusion of this study? or coming from a reference? These is no reason to have an exponential decrease in the troposphere. Many cases of thin but concentrated dust plumes transports are observed and modelled...

On average, exponentially decreasing aerosol in the troposphere is a good assumption (e.g. Gras 1991; Tomasi, 1982). This type of idealized profile is often assumed for CCN in models (e.g. Fan et al., 2007). You are correct in that individual plumes will change this profile, but here we are looking at a domain average, which regresses to the exponentially decreasing function.

l.369: "The implications for dust transport based on vertical velocities is convoluted." This sentence is difficult to understand.

This part has been further explained in the text to avoid confusion:

Ln 403-404* [The implication for dust transport based on vertical velocities is convoluted, since updrafts and downdrafts work concurrently to redistribute aerosol.]

I.421: The impact on radiation, with potential heating and cooling, is a process needing more than 2 days of simulation to be significative.

The timescales of interest vary depending on which specific processes are being examined. From a climate perspective, two days is much too short. However, looking at static stability in the lower atmosphere from a mesoscale perspective, including processes like convective initiation or the formation and deterioration of the nocturnal low-level jet, the timescales examined here (or in some cases even shorter timescales) are important and significant.

I.428: there is a sign change. Could you explain why?

The model applies a higher weight (via the refractive index for mineral dust) to dust scattering in the shortwave and cooling compared to the longwave absorption. With more dust in the explicit case, the shortwave effect is amplified.

More explanation has been added to this section for clarity:

Ln 468-470* [The model has a stronger shortwave effect for dust based on the prescribed index of refraction, but is also related to the timing of dust emissions, considering the SW effect is only active during the daytime.]

General Comments

1. There is no data used in this work: the simulations are compared between them but we have no idea of the realism of the simulations (there is only one reference for a comparison to Aeronet AOD in another paper, under discussion, and no guarantee this is exactly the same model set-up, and which one?). At least, the reference case (dx=3km) should be compared to available data (surface networks such as MIDAS, AERONET, satellite, other data).

The Saleeby et al. 2019 study (referenced above and in the paper) where the 3 km simulation was compared more thoroughly to observations has been published (once again provide the full reference here). In that paper, the exact same model setup was used for the 3 km simulation as was used here, and this point has been added to the manuscript. We have included comparison to the few AERONET sites in this region in the supplementary Fig. 12*, and found similar results (regardless of including or excluding the ICs and BCs in the simulations) with Saleeby et al. (2019) in that WRF-Chem under predicts AOD. However, the model must assume a refractive index for dust to calculate AOD, which may or may not be realistic in itself. Additionally, we have selected dust as the only aerosol present in the model, while in reality there are other aerosol types that may be contributing to the AOD. Thus, making one-to-one comparisons here with observations is difficult. None of the continuous observational networks provide dust concentration, which is what is actually needed for a true validation. Nevertheless, if WRF-Chem is underpredicting dust concentrations, this doesn't change the conclusions of the study.

2. The studied case extended from 2 to 5 August 2016: there is no spin-up time, important when studying transport of aerosol such as mineral dust. Time series are presented for the three days, but some average

are done only for the last two days, explaining that the first day is spin-up. But, viewing the domain size, the minimum spinup time should be at least one week.

See response to comment on I.178 above.

3. There is no boundary or initial conditions. These missing background values may have a large impact on the results, in particular knowing that the model couples the meteorology and the aerosol concentrations: direct and indirect aerosol effect may be long-term and it is required to have correct boundary conditions to have realistic effect of aerosol on meteorology. For the 'reference' domain, the boundary conditions are extracted from one of the studied case, biasing the results.

See response to comment on I.178 above.

4. The convection schemes used are not explained. The paper is a sensitivity study about these schemes but there is no explanations about their real differences, how they take into account aerosol or not, thus no conclusion about why results may be different depending on the scheme.

See response to comment I.177 above.

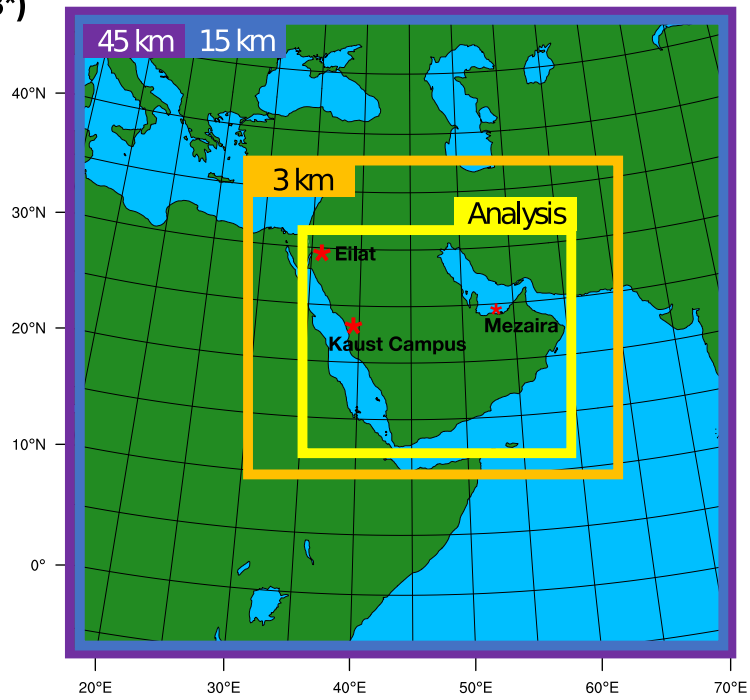
5. The paper deals with the sensitivity to the model resolution. But since the schemes are not well implemented (no wind speed distribution, no subgrid scale variability), there is a large sensitivity but not for realistic and physical reasons: the differences are not due to the convection schemes in general but just to the fact that the problem of the resolution is not well designed in this model: it is not possible to describe a threshold problem (such as mineral dust emissions) without taken into account distributions of input parameters. Results are linked to this model only and are not useful for other modellers

Regardless of how successfully or unsuccessfully these schemes have been implemented into WRF-Chem, it is still a very widely used model for air quality, atmospheric chemistry, and more relevant for our manuscript - dust research and forecasting. A list of some of the current forecasting centers using WRF-Chem can be found on the WRF-Chem users page (https://ruc.noaa.gov/wrf/wrf-chem/Real_time_forecasts.htm) and is one of the dust models included and evaluated in the SDS-WAS real-time forecasts.

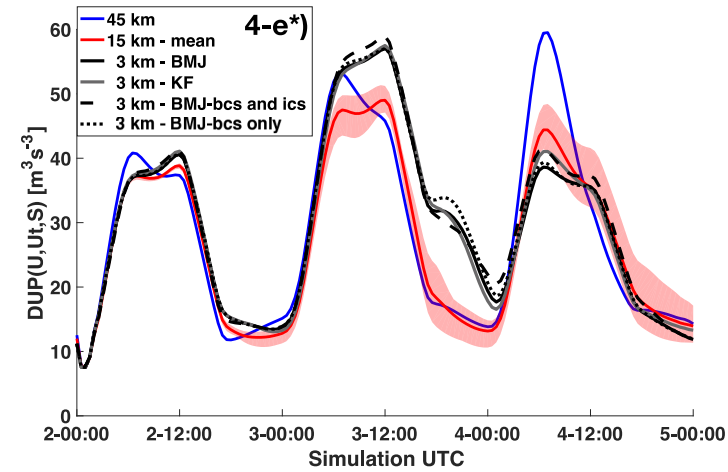
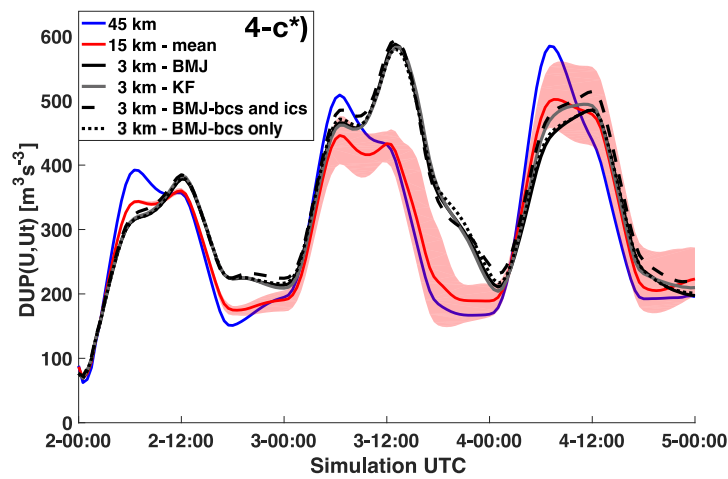
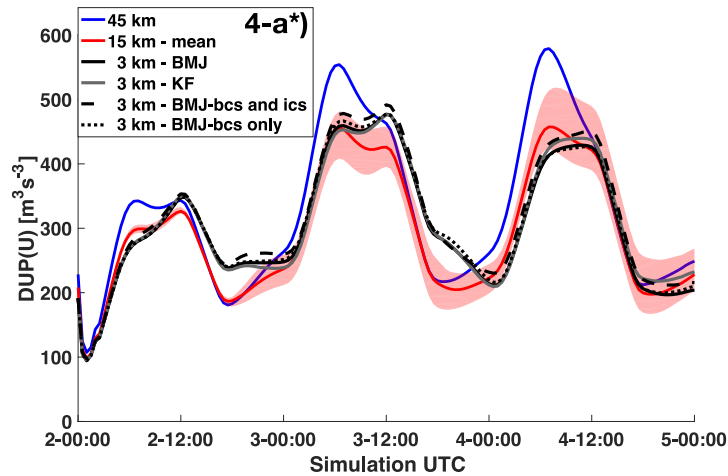
WRF-Chem users need to be aware of its limitations and its sensitivity to resolution when designing numerical experiments, and readers should be cognizant of this when interpreting results from both past and future studies that use this model. Furthermore, some of the results we found here are similar to other studies that have used different regional models, such as Reinfried et al. (2009), while other manuscripts are in disagreement with our findings, such as Heinhold et al. (2013) and Marsham et al. (2011). Clearly, we have not reached a consensus and more work is needed. Between the user base for the WRF-Chem model and the spread in results between our findings and previous literature, there is a broader community of interest for this paper.

Supplementary Figures:

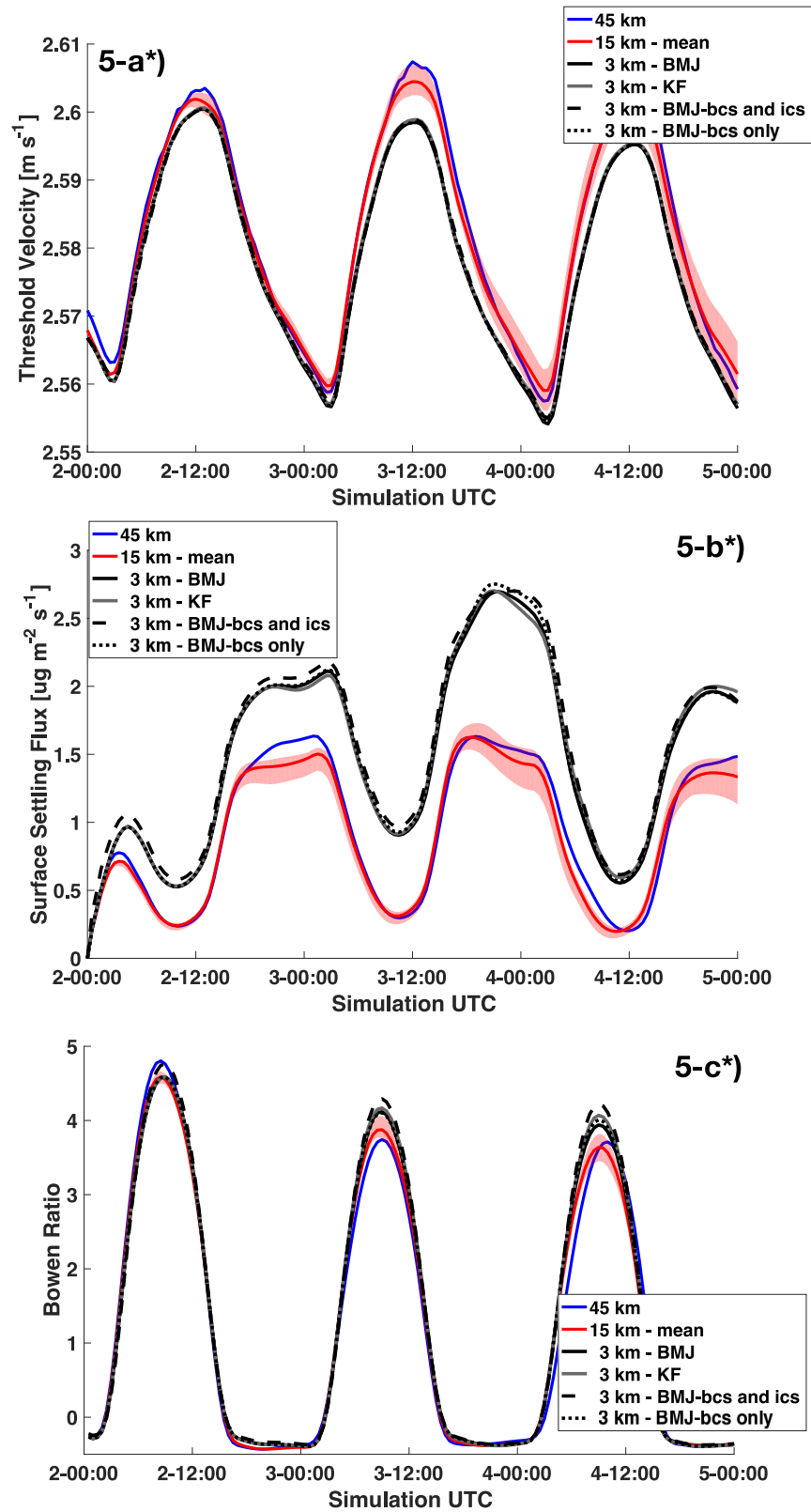
3*)



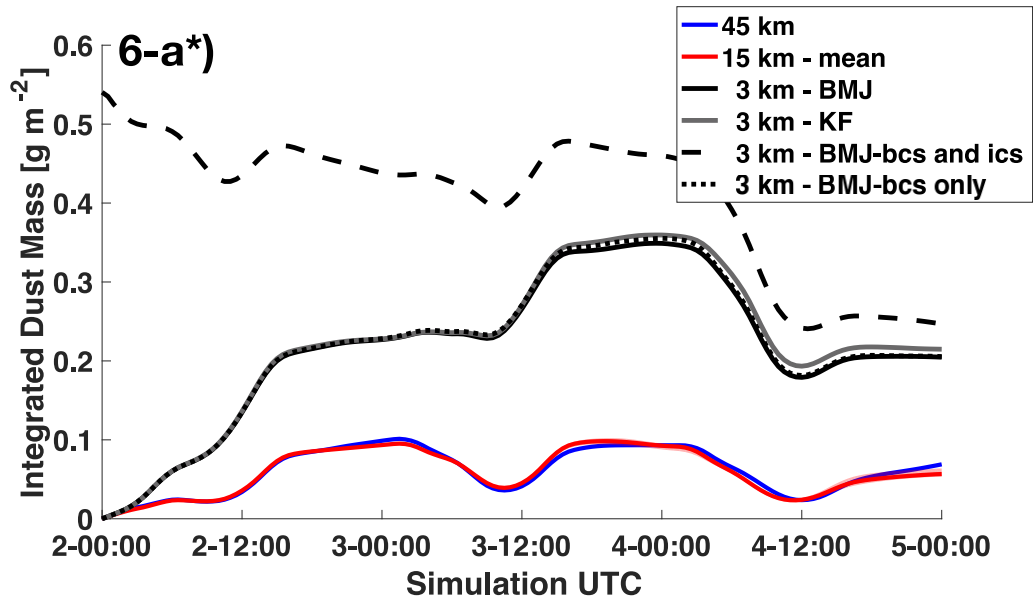
Supplementary Figure 3) Same as in Fig. 3 in the manuscript, but the location of the 3 AERONET sites in the analysis have been added.



Supplementary Figure 4A, 4C, 4E) Same as panels A, C, and E in Fig. 4 in the draft, but with 3 additional test cases: a 3 km inner nest which used the KF cumulus parameterization in its outer nest for initialization (gray solid line), a 3 km simulation with the BMJ cumulus parameterization with both initial and lateral boundary conditions for dust from the Community Atmosphere Model with Chemistry (CAM-chem) global model (black dashed line), and a 3km BMJ simulation with only the lateral boundary conditions for dust (dotted black line).

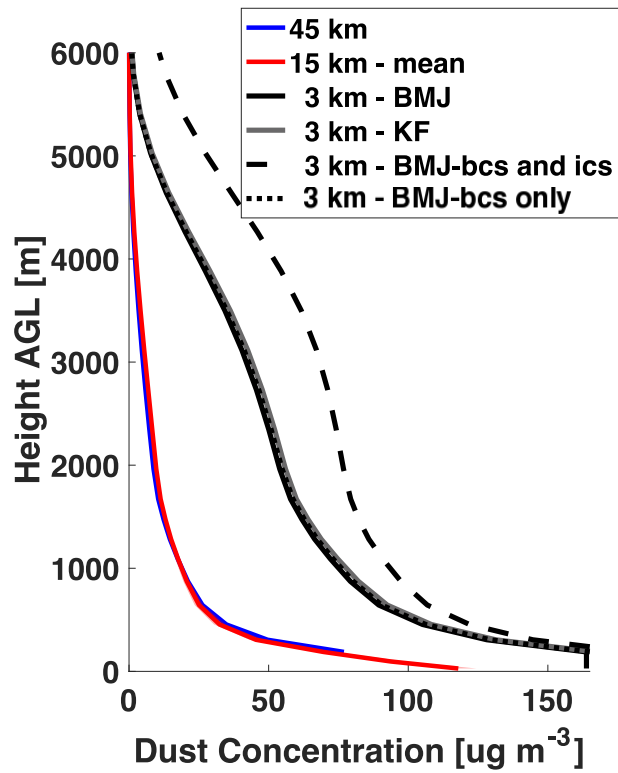


Supplementary Figure 5) Same as Fig. 5 in the draft, but with the 3 additional test cases as in Supplementary Figure 4.

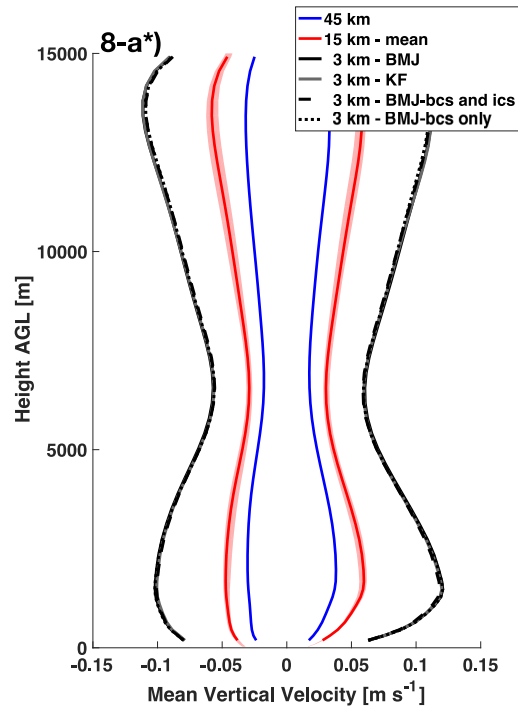


Supplementary Figure 6A) Same as panel A in Fig. 6 in the draft, but with the 3 additional test cases as in Supplementary Figure 4.

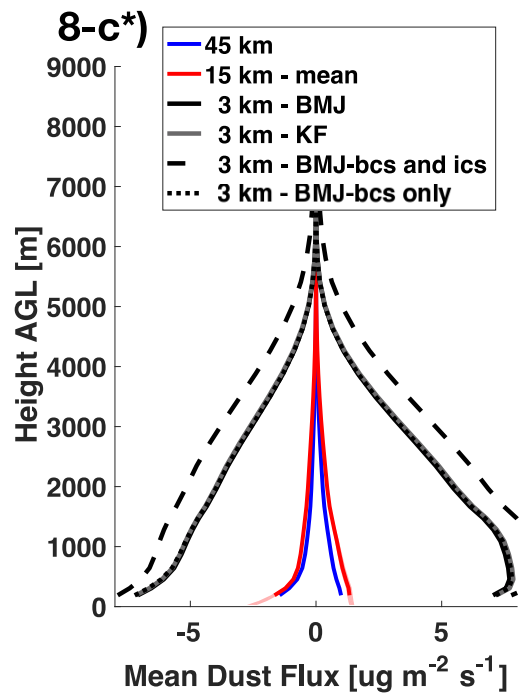
7-a*)



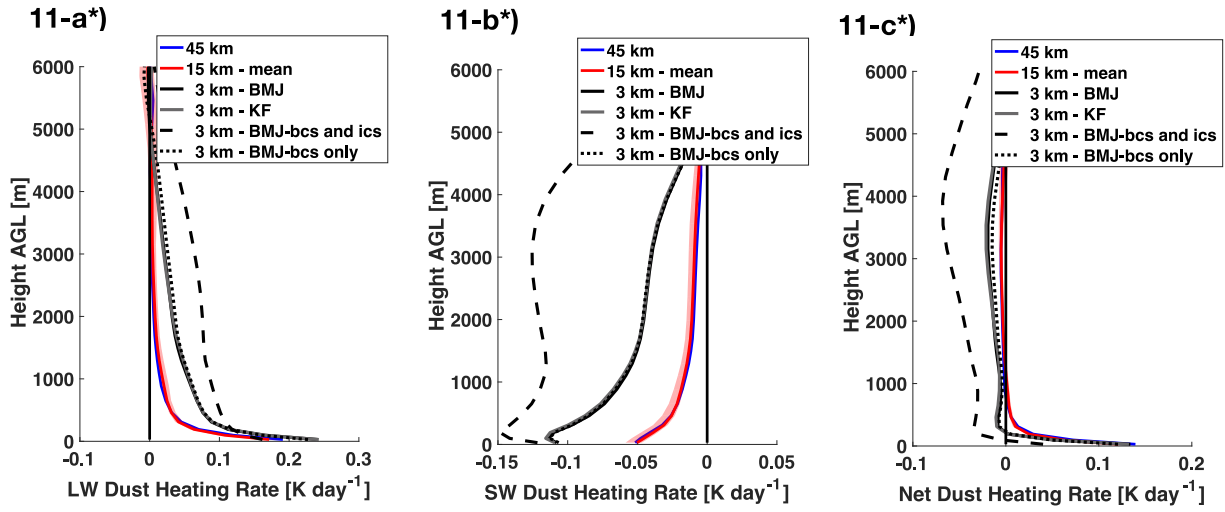
Supplementary Figure 7A) Same as panel A in Fig. 7 in the draft, but with the 3 additional test cases as in Supplementary Figure 4.



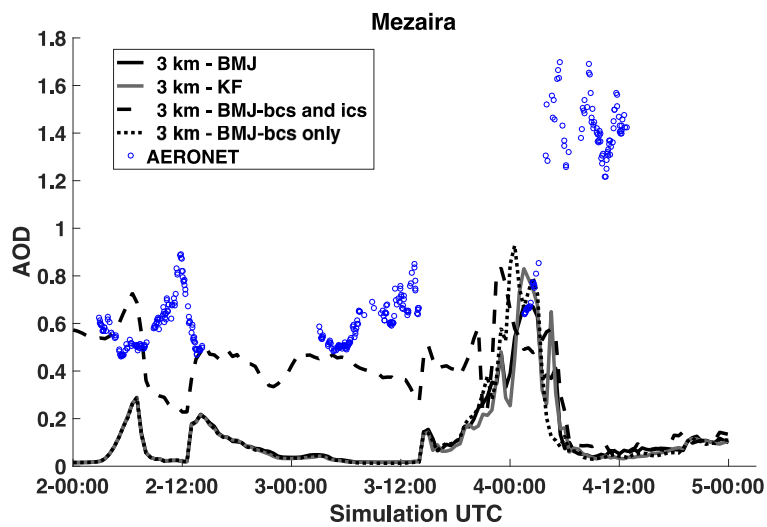
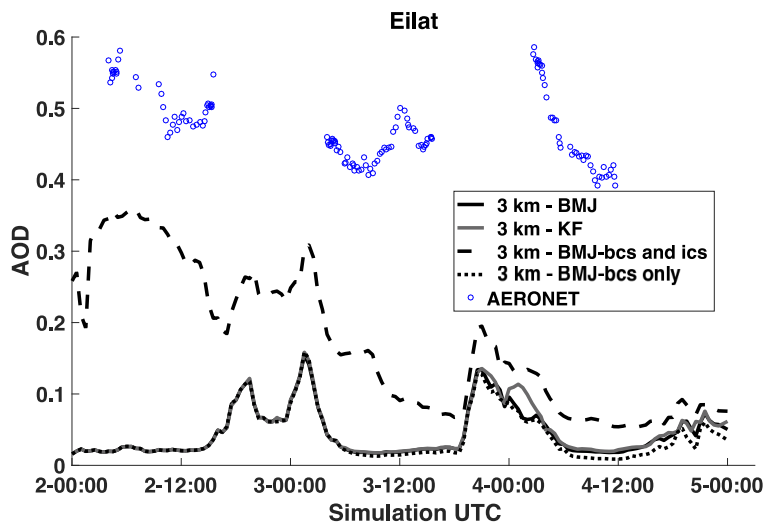
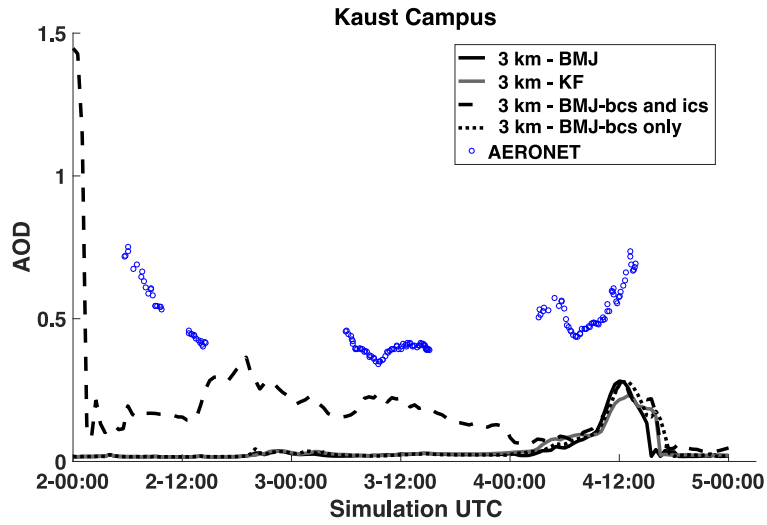
Supplementary Figure 8A) Same as Fig. 8A in the draft, but with the 3 additional test cases as in Supplementary Figure 4.



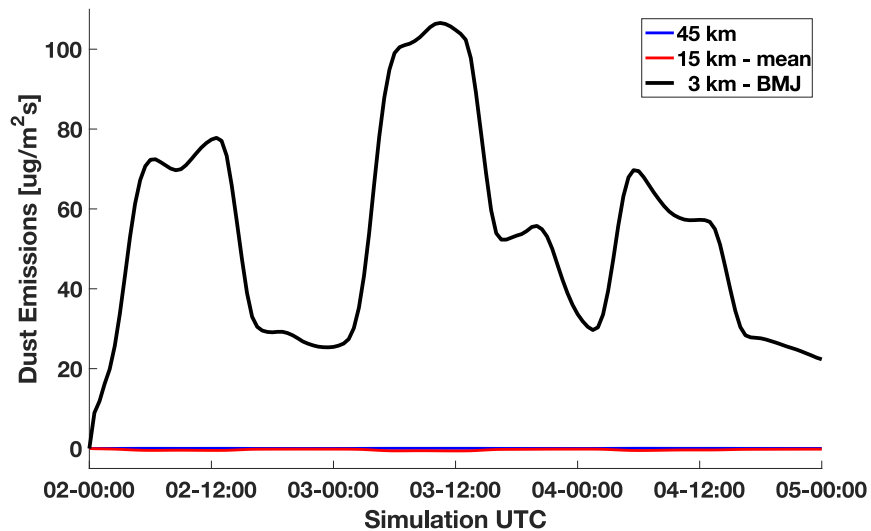
Supplementary Figure 8C) Same as Fig. 8C in the draft, but with the 3 additional test cases as in Supplementary Figure 4.



Supplementary Figure 11) Same as Fig. 11 in the draft, but with the 3 additional test cases as in Supplementary Figure 4.



Supplementary Figure 12) Comparison of the 3 km simulations modeled AOD with AERONET AOD for 3 different observational sites.



Supplementary Figure 13) Time series of dust emissions from the surface to the atmosphere.

Additional Citations

Emmons, L. K., Walters, S., Hess, P. G., Lamarque, J.-F., Pfister, G. G., Fillmore, D., Granier, C., Guenther, A., Kinnison, D., Laepfle, T., Orlando, J., Tie, X., Tyndall, G., Wiedinmyer, C., Baughcum, S. L., and Kloster, S.: Description and evaluation of the Model for Ozone and Related chemical Tracers, version 4 (MOZART-4), *Geosci. Model Dev.*, 3, 43-67, <https://doi.org/10.5194/gmd-3-43-2010>, 2010. *We acknowledge use of NCAR/ACOM CAM-chem global model output available at <https://www.acom.ucar.edu/cam-chem/cam-chem.shtml>.*

Gherboudj, I., S. N. Beegum, B. Marticorena, and H. Ghedira: Dust emission parameterization scheme over the MENA region: Sensitivity analysis to soil moisture and soil texture, *J. Geophys. Res. Atmos.*, 120, 10,915– 10,938, doi:10.1002/2015JD023338, 2015.

Gras, J. L.: Southern hemisphere tropospheric aerosol microphysics, *J. Geophys. Res.*, 96 (D3), 5345– 5356, doi:10.1029/89JD00429, 1991.

Tomasi, C.: Features of the Scale Height for Particulate Extinction in Hazy Atmospheres, *Journal of Applied Meteorology*, 21, 931-944, doi:10.1175/1520 0450(1982)021<0931:FOTSHF>2.0.CO;2, 1982.

Fan, J., R. Zhang, G. Li, W.-K. Tao, and X. Li: Simulations of cumulus clouds using a spectral microphysics cloud-resolving model, *J. Geophys. Res.*, 112, D04201, doi:10.1029/2006JD007688, 2007.

Response to RC #2

Thank you to the reviewer for their insights on the paper and research. We believe the manuscript is stronger based on their comments and we are appreciative of the thoughtful advice included here. Each comment will be addressed point by point. The * will denote line numbers in the tracked-changes manuscript.

General Comments:

I know that it is common parlance in the community to refer to simulations that are run without the use of convective parameterizations as being “explicit” or that convection is “explicitly represented”. However, more recently there has been a shift towards the use of simulations of this type being referred to as “convection permitting”. This difference is subtle but I think is a better descriptor of what the models are actually doing. The model grid-scales involved are not so fine as to explicitly resolve individual updraughts and downdraughts but are sufficiently high to permit the development of convective storms that approximate those that we might observe in reality. I feel that it would be better to replace descriptions of simulations currently described as explicit with convection permitting.

This is a very good point. We agree that the term “convection permitting” is a more accurate description of the representation of convection in the model compared “explicit.” Like the community, we have made the mistake of equalizing the two terms in the manuscript, when really only “convection permitting” should be used. The manuscript has been updated to replace “explicit” where possible with the terms “convection-permitting” and “convection-allowing.”

Did you consider running a 15 km simulation with the convective parameterization switched off. I don’t think that you should do this as the work is already of a high standard, but think that you might well be surprised at how small the difference is between a 15 km grid-spaced convection permitting simulation and a 3 km grid-spaced convection permitting simulation

We actually did run a 15 km simulation without a convective parameterization, but decided not to include the results in the manuscript. The spatial and time averaged results from the no parameterization case are, in fact, similar in magnitude to running at 15 km with a cumulus parameterization. Differences do occur in the timing of the different local dust maxima throughout the day. This points again, to resolution being the dominate factor to control in this simulation rather than the choice of cumulus parameterization (or the choice to even employ a cumulus parameterization at that grid spacing at all). A short discussion of this has been added to the manuscript:

Ln 223-224* [A 15 km simulation with no cumulus parameterization was also tested, but the results were similar and within the spread of the 15 km simulations that employed cumulus parameterizations and are not included here.]

Specific Comments:

Ln 17 -20 You need to be clear that the updraughts that are transporting dust vertically are part of the general circulation (eddies) in the dry atmosphere. At first I thought you were specifically talking about storm updraughts (which I assume are less important in the simulation for vertical dust transport due to washout).

It's a combination of both, but yes, the storm updrafts are mediated by wet deposition, whereas the dry eddies are not. This point has been included:

Ln 67-69* [Current aerosol forecast and climate models are run at fine enough grid-spacing to simulate synoptic events but still typically employ cumulus parameterizations, which are incapable of resolving dry and moist mesoscale updrafts and downdrafts that can potentially loft and / or scavenge dust.]

Ln 45-47 I think it would be wise to indicate that in reality ingestion of this type is impossible. What you are hoping for is that the initialisation data and the representation of dust are good enough for your purposes. It is perfectly possible that that is true for this case study but that the same setup run for different case studies could provide different results due to the high dependency of models (even those that do not contain dust) on initial conditions.

We agree with the reviewer's point. The spread across models (and within the same model based on physics options) can be vast. More has been included in this section to emphasize the limitations here based on model and case study choice:

Ln 47-49* [Even the state-of-the-art models are currently incapable of this type of assimilation and rely on the quality of the dust model and initialization data, which models are known to be especially sensitive to and will vary depending on the specific region and case study.]

Ln 47-49 Is it the global and regional nature of models that causes these differences or is it the grid-spacing or other model differences? Please be clear.

The dust model inter-comparison studies listed in the text varied in terms of grid resolution (horizontal and vertical) and model physics (including the dust schemes), even for the same case study. However, the grid resolution of the models was consistent in that they were all at grid-spacings that would employ a cumulus parameterization. The literature referenced here was not comparing global versus regional, but if those studies exist we are interested to see the results. The text has been updated to reduce confusion here:

Ln 49-52* [As such, substantial discrepancies exist across global models of similar resolution (Huneeus et al., 2011), and across regional models (Uno et al., 2006; Todd et al., 2008) in the magnitude of predicted dust flux from the surface to the atmosphere, as well as the models' overall representation of the dust cycle.]

Ln 50 I would get rid of "accurately" here. Generally in models dust processes are fairly simplistic and highly parameterised and so the idea that dust processes are accurately represented is a fallacy.

True, it's a stretch to say that the highly parameterized physics in the model could be thought of as "accurate". The word "accurately" has been removed from this and the next section.

Ln 53-59 This section needs rewording. The first sentence along with the word "Additionally" suggests that large-scale, synoptic-scale and meso-scale meteorology is separate from the phenomena listed below. Also why say large and synoptic scales? Instead I would suggest something like "Dust uplift events

can be associated with meteorological processes across a broad range of scales. Synoptic scale uplift phenomena include monsoon troughs (Marsham et al, Beegum et al), Shamal winds (Yu et al.) and frontal systems (Beegum et al). While dynamical effects on smaller (meso) scales can raise dust through the production of convective outflow boundaries (haboobs; Miller et al.) and the morning mixing of nocturnal low level jet (NLLJ) momentum to the surface (Fiedler et al)."

Thank you for the clarification. The wording suggested by the reviewer is a welcomed improvement and has been included in the text:

Ln 57-61* [Synoptic scale uplift phenomena include monsoon troughs (e.g. Marsham et al., 2008), Shamal winds (e.g. Yu et al., 2015) and frontal systems (e.g. Beegum et al. 2018), while dynamical effects on smaller (meso) scales can raise dust through the production of convective outflow boundaries, or haboobs, (e.g. Miller et al. 2008), daytime turbulence or dry convective processes (e.g. Klose and Shao, 2012), and the morning mixing of nocturnal low level jet (NLLJ) momentum to the surface (e.g. Fiedler et al. 2013).]

Ln 60 What other drivers of dust emission are there? There are prerequisite conditions (dry, unvegetated surface etc.) but wind is the only driver of surface dust emission that I can think of.

Possibly some anthropogenic activities can emit dust (e.g. plowing agricultural fields, construction, etc.), but ultimately, it's still then transported away from the source by the wind. This line was replaced to point out that wind is the only driver (albeit modulated by other conditions) and that we are only considering meteorological processes here:

Ln 61-62* [When considering only meteorological dust sources to the atmosphere, wind drives dust emissions...]

Ln 73 Heinold used offline emission which I think is a relevant point to mention here as it significantly differs from your approach. Another paper that discusses the grid-scale effects on online model dust and convective representation of dust in West Africa would be Roberts et al. 2018 (doi.org/10.5194/acp-18-9025-2018).

Yes, that is definitely worth mentioning and has been included. It's an important point for understanding the importance of the DUP parameter in the context of other studies. The Roberts et al. 2018 paper has also been added to the literature review to better place our results in the context of existing literature:

Ln 78-79* [Heinold et al. (2013) ran the UK Met Office Unified Model (UM) over West Africa with offline dust emissions, and found that...]

Ln 86--88* [Roberts et al. 2018 also used UM to investigate this relationship over the Sahara and Sahel and reported little change in the dust emissions when moving from parameterized to explicit convection, but also noted that the NLLJ maximum decreased as the convective maximum increased.]

Ln 82 One thing that you don't mention is that the thing that affects models the most is not the grid scale, or the microphysics and in some cases not even the whether simulations are convection permitting or parameterized. It is the initialisation data. This is one of the findings in Schepanski et al. 2015 (doi.org/10.1002/qj.2453) in West Africa.

Naturally, the model initialization data are going to be either a substantial source of error or accuracy in the output data. We have added this note and reference to the manuscript to remind readers that the findings here will be modulated by the initialization data:

Ln 70-73* [Schepanski et al. 2015 found that online dust models are likely to be most sensitive to the initialization data compared to other model options, model sensitivity to the representation of convection will be an additional source of uncertainty in dust forecasts.]

Ln 104-114 Roberts et al. 2016 (mentioned above) covers some of these points by using the Met Office Unified Model over West Africa. In the UM over summertime West Africa at least, the grid spacing does very little compared to representation of convection.

These findings have been added to the text (see above comment). But, despite the model and the region being different between these studies, we have found similar results.

Section 2.1 I find the ordering here a little odd. I would normally expect the model description to precede the description of the conditions that caused the dust uplift. It feels a little like you are skipping backwards and forwards between results and methods. I advise moving your current section 2.1 to either the end of section 2 or the start of section 3.

The case study description has been moved to the end of Section 2.

Ln 144-145 I don't think that Figs 1 and 2 show this. The first shows a number of different fields (not dust) and I wouldn't describe Figure 1 as the meteorological setup either. Figure 2 is actually 2 profiles which doesn't match the description either. Please be much clearer in you description. I cannot tell what you are referring to.

Thank you for pointing this out. We agree that it's more like a snapshot of the meteorology than an analysis of the meteorological setup. A more in-depth meteorological analysis of this case study and an attribution of the dust to different meteorological sources can be found in Miller et al. (2019) and we have directed readers there if they are interested:

Ln 258-262* [A meteorological analysis of this event, including an attribution of specific dust sources to meteorological features can be found in Miller et al., 2019 and will not be reiterated in detail here. Rather, a snapshot of the meteorology and dust fields from the WRF-Chem simulation on August 3rd at 15:00:00 UTC can be found in Fig. 1-2 as a reference to the typical meteorological setup for this case study.]

Ln 180-187 A very brief description of why these parameterizations were chosen would be welcome. For instance is this a replication of a setup used in a similar study? Is it similar to operational setups of WRF that are run for similarly arid regions? Or is there an individual reason for having chosen each of these options.

A reference was added to point out that similar WRF physics options have been used in dust studies in this region:

Ln 163-164* [The following model parameterizations were employed and kept constant across the simulations, with similar WRF physics options being utilized elsewhere to study dust effects (e.g. Alizadeh Choobari et al. 2013:)]

Ln 289 You should say why the soil moisture is more likely to fall below the threshold in the convection permitting simulations. This is very likely associated with the different way in which rainfall is generated in parameterised and convection permitting simulations. Parameterized simulations have much more widespread light rainfall while convection permitting simulations have rainfall over much smaller areas but at much higher rates. The smaller areal coverage of rainfall in the convection permitting simulations is most probably the cause of the soil moisture threshold not being exceeded as frequently.

The comment about rainfall affecting the soil moisture is on point. Thank you for raising it. We had similar ideas about this mechanism and have expanded this section to discuss these processes more.

Ln 308-313 [Rainfall is generated differently in parameterized versus convection-allowing simulations, and it has been well documented that parameterized simulations produce more widespread light rainfall, whereas more intense rainfall tends to develop over smaller areas in convection-allowing simulations (e.g. Sun et al., 2006; Stephens et al., 2010). From a domain average perspective, rainfall in the 3 km simulation will cover less area, leading to the soil moisture threshold not being exceeded as frequently compared to the parameterized cases.]

Ln 306 August 3rd

Typo has been corrected.

Ln 329 Given that Heinold and Marsham both use the UM (and I don't know what the others used but I suspect not the UM) I think you should comment on the possibility that this is a difference in model physics that is driving the different behaviour.

We have added this point throughout the manuscript to remind readers to be cognizant that the models are different and have different physics.

Ln 358-361* [...who used COSMO-MUSCAT and RAMS-DPM respectively. Considering each study used a different model and therefore physics, it is unsurprising that the results vary. However, it is not apparent how much of a role the region or specific case study plays in this difference, and is an area for future work.]

Ln 364 Once again you are not trying to explain the reason for this. In modelling of convective storms it is a well known phenomena that the radius of updraughts and downdraughts scales with the grid spacing. Could it not just be a similar effect you are seeing here. The same overall vertical motion occurs but not over such a large area (due to updraught and downdraught scaling with grid spacing) and therefore the average of grid points with non zero vertical wind speeds is relatively higher.

We agree that the scaling of the updraft / downdraft radius with grid spacing is well-known, and this is most definitely a factor here. But pushing this argument further, the finer grid spacing could permit points with higher, lower, or near-zero vertical velocities compared to the coarse spacing. The average does not necessarily have to skew higher and without testing we wouldn't know how that plays out. In

this case, the results skew to higher velocities, which is evident in the CFADs (Fig. 9). We are more likely to witness higher vertical velocities rather than lower or near-zero velocities in the 3 km simulation compared to the coarse simulations. These discussion points have been added to the section.

Ln 398-400* [It is known that in numerical models, the updraft radius scales with the grid spacing (e.g. Bryan and Morrison, 2012), with a compensating increase in updraft speed as the radius decreases. This relationship skews the frequency of vertical velocities to higher values.]

Ln 365-366 This needs to be reworded. At the moment it sounds like you are saying that the mean updraught speeds (throughout the depth of the model) are greater than the mean downdraught speeds near the surface. I suspect what you mean is that nearsurface updraughts are greater in magnitude than near-surface downdraughts (would also be nice to give a height blow which this is true).

Your interpretation is correct – the text has been updated to remove this confusion.

Ln 400-402* [Irrespective of resolution, the mean updraft speeds in the WRF-Chem simulations are slightly higher than the downdraft speeds, while at the surface mean downdraft speeds are higher than updraft speeds...]

Ln 395 “in the absence of any” ?

Discussion and recommendations and Conclusions. Do you really need both sections. There is a good deal of repetition between the two sections straight after one another. I would prefer a single Discussion and conclusions section (afterall, surely recommendations are a conclusion you arrive at from doing the work).

After considering this point, we decided to keep the sections as is and leave the result section more quantitative, with the discussion being more qualitative.

Convective distribution of dust over the Arabian Peninsula: the impact of model resolution

Jennie Bukowski¹, Susan C. van den Heever¹

¹ Department of Atmospheric Science, Colorado State University, Fort Collins, CO

Correspondence to: Jennie Bukowski (jennie.bukowski@colostate.edu)

Abstract

Along the coasts of the Arabian Peninsula, convective dust storms are a considerable source of mineral dust to the atmosphere. Reliable predictions of convective dust events are necessary to determine their effects on air quality, visibility, and the radiation budget. In this study, the Weather Research and Forecasting Model coupled with Chemistry (WRF-Chem) is used to simulate a 2016 summertime dust event over the Arabian Peninsula and examine the variability in dust fields and associated vertical transport due to the choice of convective parameterization and ~~explicit~~convection-allowing versus parameterized convection. Simulations are run at 45 km and 15 km grid spacing with multiple cumulus parameterizations, and are compared to a 3 km simulation that permits explicit ~~dry and moist~~ convective processes. Five separate cumulus parameterizations at 15 km grid spacing were tested to quantify the spread across different parameterizations. Finally, the impact these variations have on radiation, specifically aerosol heating rates is also investigated.

On average, in these simulations the ~~explicit~~convection-permitting case produces higher quantities of dust than the parameterized cases in terms of dust uplift potential, vertical dust concentrations, and vertical dust fluxes. Major drivers of this discrepancy between the simulations stem from the ~~explicit~~convection-allowing case exhibiting higher surface windspeeds during convective activity, lower dust emission wind threshold velocities due to drier soil, and more frequent, stronger vertical velocities which transport dust aloft and increase the atmospheric lifetime of these particles. For aerosol heating rates in the lowest levels, the shortwave effect prevails in the ~~explicit~~convection-permitting case with a net cooling effect, whereas a longwave net warming effect is present in the parameterized cases. The spread in dust concentrations across cumulus parameterizations at the same grid resolution (15 km) is an order of magnitude lower than the impact of moving from parameterized ~~to~~towards explicit convection. We conclude that tuning dust emissions in coarse resolution simulations can only improve the results to first-order and cannot fully rectify the discrepancies originating from disparities in the representation of convective dust transport.

1) Introduction

Airborne mineral dust is an important atmospheric aerosol (Zender et al., 2004; Ginoux et al., 2012): dust reduces visibility (e.g. Mahowald et al., 2007; Baddock et al., 2014; Camino et al., 2015) and is detrimental to the human

32 respiratory system (Prospero, 1999; van Donkelaar et al., 2010; Stafoggia et al., 2016), but also plays a vital role in
33 fertilizing iron-deficient maritime ecosystems (Martin, 1991; Bishop et al., 2002; Mahowald et al., 2005; Jickells
34 and Moore, 2015). Dust particles function as cloud condensation nuclei (e.g. Lee et al., 2009; Manktelow et al.,
35 2009; Twohy et al., 2009; Karydis et al., 2011) and ice nuclei (e.g. DeMott et al., 2003; Field et al., 2006; Knopf and
36 Koop, 2006; Boose et al., 2016), thereby altering cloud development and properties. Furthermore, mineral dust is of
37 interest due to its distinctive optical properties; dust both scatters and absorbs shortwave and longwave radiation
38 (e.g. Tegen et al., 1996; Kinne et al., 2003; Dubovik et al., 2006) modifying atmospheric thermodynamics and the
39 earth's energy budget in the process (e.g. Slingo et al., 2006; Sokolik and Toon, 2006; Heald et al., 2014).

40 The influence of atmospheric mineral dust is widespread in the weather and climate system, yet generating skillful
41 forecasts of dust concentrations and their temporal and spatial evolution has been difficult to achieve. Several
42 studies suggest that including the radiative effects of mineral dust in numerical weather prediction (NWP) could
43 refine the radiation balance of these models and improve forecasts (Kischa et al., 2003; Haywood et al., 2005; Pérez
44 et al., 2006). Advances in climate models have been made by incorporating time-varying dust sources and climate-
45 dust feedbacks in the radiative forcing calculations (Kok et al., 2014; Woodage and Woodward, 2014; Kok et al.,
46 2018). However, these potential improvements are contingent upon ingesting both ~~accurate~~ vertical dust
47 concentrations from models or observations at simulation initialization, as well as correctly representing the coupled
48 radiative effect dust has on the atmosphere. Still, Even the state-of-the-art models are currently incapable of this type
49 of assimilation and rely on the quality of the dust model and initialization data, which models are known to be
50 especially sensitive to and will vary depending on the specific region and case study. As such, -substantial
51 discrepancies exist between across global models of similar resolution (Huneus et al., 2011), and across regional
52 models (Uno et al., 2006; Todd et al., 2008) models in the magnitude of predicted dust flux from the surface to the
53 atmosphere, as well as the models' overall representation of the dust cycle.-

54 A major challenge in ~~accurately~~ modeling dust processes is the scales of motion involved in its emission and
55 subsequent transport. Dust particles mobilize from the surface due to wind erosion of arid soils, a mechanism that
56 occurs on the micron scale and must be parameterized in numerical models. Once airborne, mineral dust can deposit
57 locally or be transported on the synoptic to global scales. Dust events initiate from both large-scale and synoptic
58 dynamical flow regimes, as well as mesoscale features. Additionally, Synoptic scale uplift phenomena include
59 monsoon eirculationstroughs (e.g. Marsham et al., 2008), basin-scale pressure gradients such as the Shamal winds
60 (e.g. Yu et al., 2015), and frontal boundaries systems (e.g. Beegum et al., 2018) will produce winds strong enough
61 to emit), while dynamical effects on smaller (meso) scales can raise dust fromthrough the surface.
62 Convectiveproduction of convective outflow boundaries, also known as or haboobs, are an important source of dust
63 to the atmosphere (e.g. Miller et al., 2008), as is the early daytime turbulence or dry convective processes (e.g.
64 Klose and Shao, 2012), and the morning windspeed maximum resulting from mixing of nocturnal low-level jetsjet
65 (NLLJ) momentum to the surface (e.g. Fiedler et al., 2013). Wind is the main driver of When considering only
66 meteorological dust sources, wind drives dust emissions, meaning that the underlying processes that contribute to
67 the wind fields must be resolved in a model to create an accurate dust forecast.

68 One potential source of disagreement in models stems from the scaling emissions in dust parameterizations, which
69 relate the surface emissions proportionally to the second or third power of surface windspeed. This means that minor
70 miscalculations in modeled windspeeds go on to produce more substantial errors in the dust concentration
71 calculations (e.g. Menut, 2008). Current aerosol forecast and climate models are run at fine enough grid-spacing to
72 simulate synoptic events but still typically employ cumulus parameterizations, which are incapable of resolving
73 ~~many of the dry and moist mesoscale convective processes which~~ updrafts and downdrafts that can potentially loft
74 and / or scavenge ~~airborne~~ dust. Schepanski et al. 2015 found that online dust models are likely to be most sensitive
75 to the initialization data compared to other model options, model sensitivity to the representation of convection will
76 be an additional source of uncertainty in dust forecasts. Pope et al. (2016) and Largeron et al. (2015) both postulated
77 that ~~this~~ inadequate representation of convection in coarse model simulations, specifically the underestimation of
78 high surface windspeeds in mesoscale haboobs, is a major contributor to errors in dust models.

79
80 The misrepresentation of dust concentrations in models with cumulus parameterizations has been investigated across
81 several modeling platforms, mostly from the perspective of dust lofting mechanisms at the surface. Heinold et al.
82 (2013) ran the UK Met Office Unified Model (UM) over West Africa with offline dust emissions, and found that ~~out~~
83 of the factors they tested, the model was most sensitive to explicit versus parameterized convection. Furthermore, in
84 the Heinold et al. (2013) study, dust emissions were reduced as grid resolution was increased to convection-
85 permitting scales by roughly 50%. This was found to be due to the parameterized simulations underestimating moist
86 convective activity but drastically overestimating the NLLJ dust uplift mechanism, a similar relationship to that
87 originally identified in Marsham et al. (2011).

88 Conversely, studies using different numerical dust models have identified other relationships between horizontal
89 resolution and dust emissions. Roberts et al. 2018 also used UM to investigate this relationship over the Sahara and
90 Sahel and reported little change in the dust emissions when moving from parameterized to explicit convection, but
91 also noted that the NLLJ maximum decreased as the convective maximum increased. Reinfried et al. (2009)
92 simulated a haboob case study from Morocco with the Lokal Modell - MultiScale chemistry aerosol transport (LM-
93 MUSCAT, since renamed COSMO-MUSCAT) regional model and found increased dust emissions in ~~an explicit~~
94 convection-allowing simulation versus those with cumulus parameterizations. They also established that the model
95 was more sensitive to the choice of cumulus parameterization rather than the change in horizontal resolution.
96 Similarly, Bouet et al. (2012) identified an increase in dust emissions with increasing model resolution using the
97 Regional Atmospheric Modeling System coupled to the Dust Prediction Model (RAMS-DPM) while simulating a
98 Bodélé depression case study. Ridley et al. (2013) showed that global aerosol models with parameterized convection
99 were also sensitive to model resolution and that higher horizontal resolution led to higher dust emissions.

100
101 With the added computational expense of running aerosol code, the resolution of dust forecast models lags relative
102 to their weather-only prediction counterparts for both global and regional prediction systems (Benedetti et al., 2014;
103 Benedetti et al., 2018). Efforts have been made to advance and evaluate predictive aerosol models and ensemble
104 aerosol modeling with working groups like the International Cooperative for Aerosol Prediction (ICAP) (Benedetti

105 et al., 2011; Reid, 2011; Sessions et al., 2015), and daily dust forecasts from several aerosol models are now
106 available through the World Meteorological Organization (WMO) Sand and Dust Storm Warning Advisory and
107 Assessment System (SDS-WAS) (<http://www.wmo.int/sdswas>). Nevertheless, none of the modeling groups in the
108 SDS-WAS currently run at fine enough grid-spacing to ~~explicitly resolve~~ be considered convection-permitting (SDS-
109 WAS Model inter-comparison and forecast evaluation technical manual; last updated January, 2018). While regional
110 numerical weather prediction models have moved into convection-permitting scales, the added computational cost
111 of aerosol parameterizations means that convective parameterizations will be a necessity for longer in models that
112 employ online aerosol predictions. It is also clear that horizontal model resolution, be it specifically as to whether
113 the grid-spacing is fine enough to permit the explicit resolution of convective processes or is coarse enough to
114 mandate parameterized convection, is also still an understudied factor in regional dust modeling. As such, exploring
115 differences across cumulus parameterizations and those relative to convection-permitting resolutions remains
116 relevant and vital to better understand aerosol forecasting and aerosol-cloud-environment interactions.

117 While previous studies have begun to examine the effect of horizontal model resolution on dust emissions and
118 airborne dust concentrations, there are several factors that warrant more investigation. As it stands, there is little
119 agreement on the sign of the response in dust emissions to a change in model resolution, which seems to vary based
120 on the regional model being utilized. Most studies have concentrated on the change in dust emissions based on
121 moving from parameterized convection to ~~explicit~~ convection-allowing scales, while ignoring the possible
122 sensitivity due to the choice of the cumulus parameterization itself. Furthermore, much of the previous literature
123 focused on how the increase in resolution affects convective outflow boundaries and surface / near-surface processes
124 as dust sources, rather than convective transport and the vertical redistribution of dust and its radiative effects at
125 different levels of the atmosphere. In this paper, we seek to address these limitations in the understanding of the
126 effects of horizontal model resolution on dust concentrations. The goal of the research presented here is therefore to
127 quantify the sign and magnitude in the response of modeled dust fields in a regional numerical model to increasing
128 horizontal resolution.

129 In order to achieve our stated goal, we will use numerical simulations of a case study to examine the variability in
130 dust emissions and vertical dust concentrations and fluxes due to (1) the choice of convective parameterization, (2)
131 ~~explicit~~ convection-allowing versus parameterized convection, and (3) the impact of these variations on radiation,
132 specifically aerosol heating rates. These simulations are performed using the Weather Research and Forecasting
133 Model coupled with Atmospheric Chemistry (WRF-Chem) (Skamarock et al., 2008; Grell et al., 2005; Fast et al.,
134 2006) a platform that has been tested for its sensitivity to vertical resolution for dust extinction coefficient profiles
135 (Teixeira et al., 2015) and horizontal model resolution and convective transport for chemical species such as carbon
136 monoxide (e.g. Klich and Fuelberg, 2013), but not for dust. These simulations will represent a case study of a
137 summertime coastal convective dust event over the Arabian Peninsula, a relatively understudied region compared to
138 areas such as the Sahara (Jish Prakash et al., 2015), despite being the world's second largest dust emission region
139 (Tanaka and Chiba, 2004).

140 This paper is part of a larger body of collaborative work conducted by the Holistic Analysis of Aerosols in Littoral
141 Environments (HAALE) research team under the Office of Naval Research Multidisciplinary Research Program of
142 the University Research Initiative (MURI). The primary goal of the HAALE-MURI project is to isolate the
143 fundamental environmental factors that govern the spatial distribution and optical properties of littoral zone aerosols.
144 The study discussed in this manuscript focuses on advancing our understanding in the role that convection plays in
145 the redistribution of dust aerosol and its radiative effects along the coast of arid regions, and seeks to quantify the
146 uncertainty in forecasted dust distributions stemming from the representation of convective processes in a regional
147 model.

148 The manuscript is organized as follows: an overview of the ~~case study is found in Sect. 2.1, followed by the~~ WRF-
149 Chem model and physics setup (Sect. 2.21), dust model setup (Sect. 2.32), information about the cumulus
150 parameterizations and model resolution (Sect. 2.43), and analysis methods in Sect. 2.4. ~~A description of the case~~
151 ~~study is found in Sect.~~ 2.5. The results are outlined in Sect. 3, with a discussion on the temporal evolution of dust
152 concentrations and dust uplift potential in Sect. 3.1, vertical distributions and fluxes of dust in Sect. 3.2, and the
153 effect on aerosol radiative heating rates in Sect. 3.3. A discussion of the results and implications for the community
154 are located in Sect. 4 and a summary of the findings of this study are reviewed in Sect. 5.

155 2) Case study and model description

156 2.1) ~~Case study overview~~

157 ~~The dust event simulated for this study occurred during August 2-5, 2016 across the Arabian Peninsula, and~~
158 ~~originated from a combination of synoptic and mesoscale dust sources. An example of the meteorological setup and~~
159 ~~dust fields for this case study can be found in Fig. 1-2. For this event, the high summertime temperatures in the~~
160 ~~desert of the Arabian Peninsula produce a thermal low couplet at the surface, with one low centered over Iraq and~~
161 ~~the other over the Rub' al Khali desert in Saudi Arabia (Fig. 1.e). The local low pressure couplet leads to cyclonic~~
162 ~~surface winds between these two areas (Fig. 1.e), comprised of northerly flow from Iraq into Saudi Arabia, with~~
163 ~~returning southerly flow from Oman over the Persian Gulf and into Kuwait, and is a major non-convective~~
164 ~~contributor to the dust budget for this case study (Fig. 1.f). In addition to these large-scale flow patterns, a daytime~~
165 ~~sea breeze brings moist, maritime air from the coast of Yemen and Oman inland into the otherwise arid Saudi~~
166 ~~Arabian basin (Fig. 1.e and 1.d). This moisture gradient is also evident in the skew-t diagrams, which represent an~~
167 ~~inland radiosonde release site at Riyadh (Fig. 2.a), and a site closer to the coast in Abha (Fig. 2.b), both located in~~
168 ~~Saudi Arabia. There is a stark difference in low-level moisture between the two sites, although both display a~~
169 ~~subsidence inversion aloft between 500 and 600 hPa. Furthermore, nocturnal low-level jets form along the Zagros~~
170 ~~mountains in Iran and Iraq, and the Red sea, both of which have been studied previously in the literature~~
171 ~~(Giannakopoulou and Toumi, 2011; Kalenderski and Stenchikov, 2016).~~

172 ~~Due to the region's inherent moisture constraints, convection is limited spatially to the coastal regions of the~~
173 ~~Arabian Peninsula, as is most summertime convective and non-convective precipitation in this region (e.g. Shwchdi,~~

2005; Almazroui, 2011; Hasanean and Almazroui, 2015; Babu et al., 2016). Moist convective cells develop along a low level convergence line between the northerly basin flow and sea breeze front (Fig. 1.g and 1.h) aided by elevated terrain in Yemen and Oman (Fig. 1.a). This convective setup along the southern portion of the Arabian Peninsula is a feature evident in each day of this case study, initializing diurnally in the local late afternoon and early evening, and thereby providing three days of data for analysis, with the height of convective activity occurring on August 3rd. Individual convective cells form along the convergence line, a typical Middle Eastern characteristic (Dayan et al., 2001), but do not organize further, owing to a lack of upper level synoptic support and insufficient moisture in the interior of the peninsula. Nevertheless, the convective line does produce outflow boundaries, which loft dust from the surface and are the main convective dust source for this case study. More information on the meteorological setup of this case study, including comparisons with aerosol optical depth (AOD) observations can be found in Saleeby et al. (2019).

2.2) WRF-Chem model description and physics

To investigate the Arabian Peninsula case study, WRF-Chem version 3.9.1.1 is used to simulate the dust outbreak meteorology and aerosol fields. WRF-Chem is an online numerical chemical transport model that allows for interactive aerosol processes, including feedbacks between the meteorology, aerosol, and radiation. The model is coupled to the Goddard Chemistry Aerosol Radiation and Transport (GOCART) module (Ginoux et al., 2001), which ~~will be~~allows for feedbacks between the meteorology and aerosols and is described in more detail in Sect. 2.3~~2~~.

The meteorological and sea surface temperature initial and lateral boundary conditions are sourced from the 0.25 degree, 6-hourly Global Data Assimilation System Final Analysis (GDAS-FNL). No chemistry or aerosol initial / lateral boundary conditions are used. Rather, the aerosol fields are initialized with zero concentrations and are allowed to evolve naturally from the model meteorology, aerosol, surface and radiation processes. The model is run from 00:00:00 UTC on 02-Aug-2016 to 00:00:00 UTC on 05-Aug-2016 producing output at 30-minute intervals. The following model parameterizations were employed and kept constant ~~throughout the simulations; across the simulations, with similar WRF physics options being utilized elsewhere to study dust effects (e.g. Alizadeh Choobari et al. 2013)~~; Morrison double-moment microphysics (Morrison et al., 2005; 2009), RRTMG longwave scheme (Iacano et al., 2008), Goddard shortwave radiation scheme (Chou and Suarez, 1999), the Noah Land Surface Model with multiparameterization options (Niu et al., 2011; Yang et al., 2011), and the MYNN level 3 boundary layer parameterization (Nakanishi and Niino, 2006; 2009). The convective parameterizations and horizontal resolutions tested will be discussed in Sect. 2.4. A summary of the physics options utilized can be found in Table 1.

2.3~~2~~) GOCART dust emissions and dust uplift potential

WRF-Chem is coupled to the GOCART dust module, which parameterizes the emission of dry mineral dust mass from the surface to the atmosphere for 5 effective radii bins [0.5, 1.4, 2.4, 4.5, and 8.0 μm] based on Eq. (1):

$$F_p = CS_s U^2 (U - U_t) \text{ if } U > U_t \quad (1)$$

208 In Eq. (1), F_p is the dust flux from the surface [$\text{kg m}^{-2} \text{s}^{-1}$] for each of the radii bins (p), S represents the wind erosion
 209 scaling factor [0 to 1] established by the Ginoux et al. (2004) soil erodibility map, s_p is the fraction of each size class
 210 within the soil [0 to 1] based on the silt and clay fraction of the soil type, U is the 10 m wind speed [m s^{-1}], and U_t is
 211 the threshold velocity of wind erosion [m s^{-1}]. C is a tuning constant (set here to a default $1 \text{ kg s}^2 \text{ m}^{-5}$), which can be
 212 set by the user to increase or decrease the total dust flux based on regional observations (e.g. Zhao et al., 2010;
 213 Kalenderski et al., 2013; Dipu et al., 2013). If the wind speed is less than the threshold velocity, no dust will loft
 214 from the surface. Most of the terms in Eq. (1) are time invariant (C, S, s_p), except for the wind speed (U) and wind
 215 erosion threshold (U_t). U_t is a function of soil wetness, and is calculated with the relationship found in Eq. (2):

$$216 \quad U_t = \begin{cases} 6.5 \sqrt{\frac{\rho_p - \rho_a}{\rho_a}} g D_p (1.2 + \log_{10} w_{soil}) & \text{if } w_{soil} < 0.5 \\ \infty & \text{if } w_{soil} \geq 0.5 \end{cases} \quad (2)$$

217 For Eq. (2), ρ_p is the dust particle density [kg m^{-3}], ρ_a is the density of air [kg m^{-3}], g is gravitational acceleration [m
 218 s^{-2}], and w_{soil} is the soil wetness fraction [0 to 1]. Similar to Eq. (1), Eq. (2) includes a threshold, whereby above a
 219 soil wetness of 0.5, no dust will be emitted. If the threshold criteria are met and dust lofts from the surface, it is then
 220 transported based on the simulated meteorological fields from WRF, including advection, convection, and turbulent
 221 mixing, and is removed from the atmosphere via gravitational settling and wet deposition. Here, wet deposition is
 222 included as a scavenging mechanism to provide a more realistic picture of the convective moist convection transport
 223 process. Aerosol radiation interactions in the shortwave and longwave (Barnard et al., 2010) are included in the
 224 simulations to understand the implications that lofted dust has on the energy budget of the case study and are
 225 discussed in Sect. 3.3.

226 Before dust can amass in and influence the atmosphere, it must first be emitted from the surface. Because of the
 227 threshold values included in the GOCART dust parameterization equations (Eq. 1-2), it is important to understand
 228 how often the modeled near-surface wind speeds exceed the wind threshold value. A parameter useful in describing
 229 the influence of the wind on dust emissions is Dust Uplift Potential (DUP), proposed by Marsham et al. (2011) and
 230 based on Marticorena and Bergametti (1995). The DUP parameter is an offline approximation for the relative
 231 amount of dust expected to loft from the surface. DUP is a convenient way to perform first order sensitivity tests on
 232 the meteorology without having to re-run the model, and provides a framework for deconvolving the variables in Eq.
 233 (1-2). Here, we have adapted the DUP parameter from Marsham et al. (2011) (Eq. 4) into three variations (Eq. 3-5),
 234 which allows researchers to vary the complexity of the analysis by including more, or fewer degrees of freedom.

$$235 \quad DUP(U) = U^3 \left(1 + \frac{A}{U}\right) \left(1 - \frac{A^2}{U^2}\right) \quad (3)$$

$$236 \quad DUP(U, U_t) = U^3 \left(1 + \frac{U_t}{U}\right) \left(1 - \frac{U_t^2}{U^2}\right) \quad (4)$$

$$237 \quad DUP(U, U_t, S) = S U^3 \left(1 + \frac{U_t}{U}\right) \left(1 - \frac{U_t^2}{U^2}\right) \quad (5)$$

238 In Eq. (3), U_t is set to a constant wind speed, A , thereby making DUP a function of only the near-surface wind
239 speed; for the purpose of this paper U_t is set to 5 m s^{-1} , but has been tested elsewhere across the range of $5\text{-}10 \text{ m s}^{-1}$
240 (e.g. Marsham et al., 2011; Cowie et al., 2015; Pantillon et al., 2015). This simplified equation for dust uplift has
241 been used in previous dust studies, and is useful to include here to place this manuscript in the context of existing
242 literature. Eq. (4) is slightly more intricate in that it considers the model evolution of U_t due to changing soil wetness
243 from precipitation and land-surface processes, calculated by Eq. (2). Lastly, Eq. (5) builds on Eq. (4) by including
244 the soil erodibility scaling factor (S), which recognizes that the U and U_t relationship is valid only if it occurs over
245 potential dust source regions. Since U , U_t , and S are entangled in the GOCART dust parametrization found in Eq.
246 (1-2), the seemingly minor variations between the DUP parameters in Eq. (3-5) are crucial for isolating which
247 processes, or combination of processes, are sensitive to the horizontal resolution of the model, and hence to the
248 analysis performed here.

249 **2.43) Domain, nesting, and cumulus parameterizations**

250 Several horizontal model grid-spacings (45 km, 15 km, and 3 km) of the Arabian Peninsula domain (Fig. 3) ~~are~~were
251 tested to identify the sensitivity of modeled dust concentrations to the model's horizontal resolution. For the two
252 coarsest simulations (45 km and 15 km), cumulus parameterizations ~~are~~were employed to represent shallow and
253 deep convection. The 45 km simulation was run with only the Betts–Miller–Janjic (BMJ) cumulus parameterization
254 (Janjic, 1994), while five different cumulus parameterizations were tested for the 15 km simulations, including the
255 BMJ, Kain–Fritsch (KF) (Kain, 2004), Grell 3D Ensemble (GD) (Grell, 1993; Grell et al., 2002), Tiedtke (TD)
256 (Tiedtke, 1989; Zhang et al., 2011), and Simplified Arakawa–Schubert (AS) (Arakawa and Schubert, 1974; Han and
257 Pan, 2011) schemes, which will determine the sensitivity of dust lofting to different cumulus parameterizations. A
258 15 km simulation with no cumulus parameterization was also run, but the results were similar and within the spread
259 of the 15 km simulations that employed cumulus parameterizations and are not included here. The finest resolution
260 simulation (3 km) ~~is~~was run at convection-permitting scales and hence no cumulus parameterizations were invoked.
261 The 3 km simulation ~~is~~was initialized as a one-way nest ~~initialized~~ from the 15 km BMJ simulation which
262 ~~services~~served as its parent lateral boundary conditions. Other combinations of nests were tested, but the results were
263 not sensitive to which 15 km simulation was used as the parent nest, or lateral boundary conditions, for the 3 km
264 simulation. A summary of the model domains is also found in Fig. 3.

265 The cumulus parameterizations tested in this study for the 15 km simulations vary in their methods for triggering
266 and then characterizing convective processes at the sub-grid scale level. BMJ is a moisture and temperature
267 adjustment scheme that acts to restore the pre-convective unstable thermodynamic profile to a post-convective stable
268 and well-mixed reference profile, while the other cumulus parameterizations (KF, GD, TD, AS) employ a mass-flux
269 approach to determine updraft and downdraft mass transport. Across the mass-flux parameterizations, GD is unique
270 in that it computes an ensemble of varying convective triggers and closure assumptions and then feeds the ensemble
271 mean back to the model. Furthermore, all five schemes represent shallow convection in addition to deep convection,
272 the mass-flux schemes include detrainment of water and ice at cloud top, and AS and TD are formulated to include
273 momentum transport in their calculations. These differences across parameterizations will result in varying updraft

274 and downdraft speeds and precipitation rates, which will have consequences for the vertical transport of airborne
275 dust, as well as the strength of convective outflow boundaries and therefore dust emission at the surface.

276 **2.54) Averaging and analysis methods**

277 Because the representation of convective processes varies across the simulations, the results will focus on composite
278 statistics from the three-day case study. The authors make no attempt to track and match individual convective
279 elements across simulations, as their triggering, timing, and development (or lack of development) will fluctuate
280 depending on the model resolution and cumulus parameterization, thus making a truly consistent analysis
281 problematic. Instead, this paper takes a step backward and aims to quantify in an average sense, how the choice of
282 horizontal resolution and parameterized convection affects dust concentrations in the WRF-Chem model across the
283 Arabian Peninsula. The analyses and averages are processed within the yellow box shown in Fig. 3, disregarding all
284 other grid points outside the Arabian Peninsula study area. Analyses that are averaged in time are only averaged
285 over the last two days of the simulation (00:00:00 UTC on 03-Aug-2016 to 00:00:00 UTC on 05-Aug-2016) to
286 account for model spin up in the first 24 hours. All results are summed over the five dust bins in the GOCART
287 model rather than being treated separately. Lastly, the results from the five 15 km simulations are averaged together
288 to produce a mean 15 km resolution response, and is presented, along with the maximum and minimum spread
289 across these simulations for reference.

290

291

292 **2.5) Case study overview**

293 The dust event simulated for this study occurred during August 2-5, 2016 across the Arabian Peninsula, originating
294 from a combination of synoptic and mesoscale dust sources. A meteorological analysis of this event, including an
295 attribution of specific dust sources to meteorological features can be found in Miller et al., 2019 and will not be
296 reiterated in detail here. Rather, a snapshot of the meteorology and dust fields from the WRF-Chem simulation on
297 August 3rd at 15:00:00 UTC can be found in Fig. 1-2 as a reference to the typical meteorological setup for this case
298 study.

299 For this event, the high summertime temperatures in the desert of the Arabian Peninsula produce a thermal low
300 couplet at the surface, with one low centered over Iraq and the other over the Rub' al Khali desert in Saudi Arabia
301 (Fig. 1.c). The local low-pressure couplet leads to cyclonic surface winds between these two areas (Fig. 1.e),
302 comprised of northerly flow from Iraq into Saudi Arabia, with returning southerly flow from Oman over the Persian
303 Gulf and into Kuwait, and is a major non-convective contributor to the dust budget for this case study (Fig. 1.f). In
304 addition to these large-scale flow patterns, a daytime sea breeze brings moist, maritime air from the coast of Yemen
305 and Oman inland into the otherwise arid Saudi Arabian basin (Fig. 1.e and 1.d). This moisture gradient is also

306 evident in the skew-t diagrams, which represent an inland radiosonde release site at Riyadh (Fig. 2.a), and a site
307 closer to the coast in Abha (Fig. 2.b), both located in Saudi Arabia. There is a stark difference in low-level moisture
308 between the two sites, although both display a subsidence inversion aloft between 500 and 600 hPa. Furthermore,
309 nocturnal low-level jets form along the Zagros mountains in Iran and Iraq, and the Red sea, both of which have been
310 studied previously in the literature (Giannakopoulou and Toumi, 2011; Kalenderski and Stenchikov, 2016).

311 Due to the region's inherent moisture constraints, convection is limited spatially to the coastal regions of the
312 Arabian Peninsula, as is most summertime convective and non-convective precipitation in this region (e.g. Shwehdi,
313 2005; Almazroui, 2011; Hasanean and Almazroui, 2015; Babu et al., 2016). Moist convective cells develop along a
314 low-level convergence line between the northerly basin flow and sea breeze front (Fig. 1.g and 1.h) aided by
315 elevated terrain in Yemen and Oman (Fig. 1.a). This convective setup along the southern portion of the Arabian
316 Peninsula is a feature evident in each day of this case study, initializing diurnally in the local late afternoon and early
317 evening, and thereby providing three days of data for analysis, with the height of convective activity occurring on
318 August 3rd. Individual convective cells form along the convergence line, a typical Middle Eastern characteristic
319 (Dayan et al., 2001), but do not organize further, owing to a lack of upper-level synoptic support and insufficient
320 moisture in the interior of the peninsula. Nevertheless, the convective line does produce outflow boundaries, which
321 loft dust from the surface and are the main convective dust source for this case study. More information on the
322 meteorological setup of this case study, including comparisons with aerosol optical depth (AOD) observations can
323 be found in Saleeby et al. (2019).

324 **3) Results**

325 **3.1) Temporal evolution**

326 **3.1.1) Dust uplift potential**

327 The first process of interest in determining the sensitivity of modeled dust concentrations to horizontal resolution in
328 WRF-Chem is the amount of dust lofted from the surface to the atmosphere. Fig. 4 depicts the average DUP for the
329 simulations at each 30-minute output, using Eq. (3-5) to separate out the importance of the different mechanisms
330 regulating dust emissions.

331 Regardless of which DUP parameter is used, almost all of the simulations capture the bimodal daily maximum in
332 dust emissions in the local mid-morning (6 UTC) and late afternoon (13 UTC) due to the mixing of the NLLJ to the
333 surface and convective outflow boundaries, respectively. The only resolution where the bimodality is absent is the
334 45 km simulation, which captures the NLLJ mechanism, but misses the second convective activity maximum. The
335 coarsest simulation overestimates the NLLJ-near-surface wind speeds related to the NLLJ mechanism, which
336 subsequently inhibits convection later in the day. Because of this, the 45 km simulation has the highest DUP(U)
337 (Fig. 4.a) based only on wind speed (Eq. 3), a result similar to the Heinhold et al. (2013) and Marsham et al. (2011)
338 studies over the Sahara.

339 However, when taking the calculated threshold wind velocity into account (Eq. 4), the ~~explicit~~convection-allowing
340 simulation (3 km) displays the strongest DUP(U, U_t) at the local late afternoon convective maximum (Fig. 4.c). For
341 this to be the case compared to the DUP(U) parameter, the 3 km simulation must have a lower threshold wind
342 velocity (Fig. 5.a) than the simulations with parameterized convection. Since the threshold wind velocity is
343 proportional to soil wetness (Eq. 2), this implies that the ~~explicit~~convection-permitting simulation will on average
344 have drier soil, or more grid points below the soil wetness threshold than the parameterized simulations. ~~The effects~~
345 ~~of~~Rainfall is generated differently in parameterized versus convection-allowing simulations, and it has been well
346 documented that parameterized simulations produce more widespread light rainfall, whereas more intense rainfall
347 tends to develop over smaller areas in convection-allowing simulations (e.g. Sun et al., 2006; Stephens et al., 2010).
348 From a domain average perspective, rainfall in the 3 km simulation will cover less area, leading to the soil moisture
349 threshold not being exceeded as frequently compared to the parameterized cases.

350 This spatial difference in rainfall leads to the 3 km case having drier soil ~~are indeed~~on average across the domain,
351 which is evident in the surface fluxes ~~with~~represented by the Bowen ratio of sensible to latent heat fluxes in Fig. 5.c.
352 When the Bowen ratio is above one, more of the surface heat exchange with the atmosphere is in the form of
353 sensible heat flux, rather than latent heat flux. Dry soils are characterized by low values of latent heat flux, and
354 therefore exhibit higher Bowen ratios. The 3 km simulation exhibits a higher Bowen ratio on August 3rd and 4th,
355 indicating that the soil is on average drier in the ~~explicit~~convection-permitting simulation. This result implies that
356 disparities in land surface properties across the varying model grid resolutions are important for modulating dust
357 emissions, both from the perspective of ~~explicit~~convection-allowing versus parameterized convection and associated
358 precipitation, as well as latent and sensible heat fluxes.

359 Adding on to the complexity of the DUP parameter, when the location of dust sources is considered in the
360 DUP(U, U_t, S) calculations (Eq. 5), some of variability between the local NLLJ and convection maxima is lost in the
361 3 km simulation (Fig. 4.e) on August 3rd. Also, including the scaling factor reduces the magnitude of the DUP
362 parameter to roughly 10% of the initial values for DUP(U) and DUP(U, U_t). Incorporating the dust source function in
363 DUP works not only as a scaling factor for the magnitude of potential dust emissions, but also impacts the relative
364 importance of dust production mechanisms (NLLJ versus convection). This shift is a consequence of the location in
365 which these processes occur. For instance, the reduction in the 3 km convective maximum on August 3rd between
366 DUP(U, U_t) and DUP(U, U_t, S) signifies that convection is occurring in locations that are not active dust source
367 regions. Without information on the dust source regions, this process would be assigned an unrealistic dominance
368 over the NLLJ mechanism in terms of DUP.

369 All simulations are similar for the first 24 spin-up hours until the processes begin to diverge on August 3th3rd, where
370 the ~~explicit~~convection-allowing simulation produces the maximum DUP(U, U_t, S) both during the local daytime and
371 nighttime hours. On the final day of the case study (August 4th), the ~~explicit~~convection-allowing simulation has the
372 lowest DUP(U, U_t, S), with the NLLJ maximum dominating over the convective maximum in both the 3 km and the
373 15 km mean, due to reduced convective activity in the fine resolution simulations. Examining the percent difference

374 in DUP between the coarse and fine simulations (Fig. 4.b,d,f), the average percent difference between the 3 km and
375 15 km simulations is at a minimum when only wind speed is considered, and increases as the degrees of freedom in
376 DUP increases. For the DUP(U,U_t,S) case, the average percent difference is between 10-65% lower in the 15 km
377 simulations than the explicitconvection-permitting simulation, with a maximum difference of 85% and a spread
378 across parameterizations of 20%. This implies that the explicitconvection-allowing WRF-Chem simulation has the
379 potential to loft up to 85% more dust than those with parameterized convection.

380 3.1.2) IntegratedVertically integrated dust mass

381 The differences in DUP(U,U_t,S), or dust flux from the surface to the atmosphere, specifically the enhanced values
382 for the explicitconvection-permitting simulation on August 3rd, will lead to more dust lofting than in the coarse
383 simulations. To see how differences in the dust emissions translate into differences in airborne concentrations of
384 dust, Fig. 6 demonstrates the temporal evolution of the averagespatially averaged, vertically integrated dust mass
385 throughout the vertical column. Here, the explicitconvection-allowing simulation records upwards of 150% more
386 integrated dust mass compared to the coarse resolution simulations. Across the coarse simulations, the 45 km and 15
387 km runs have similar vertically integrated dust magnitudes, despite the temporal differences in DUP(U,U_t,S). This is
388 due to the overestimation of the NLLJ in the 45 km simulations being offset by the enhanced convective dust lofting
389 in the 15 km simulations.

390 The discrepancy in the diurnal maxima across horizontal resolutions is similar to the results of the UM in Marsham
391 et al. (2011) and Heinhold et al. (2013). Yet, the results here differ in that both of these previous studies found a
392 stronger NLLJ response in 12 km simulations with convective parameterizations than was found here in the 15 km
393 parameterized ensemble. In contrast to the findings of Marsham et al. (2011) and Heinhold et al. (2013), dust
394 emissions and airborne dust mass increases in the WRF-Chem simulations as resolution increases in the convection-
395 allowing simulation, which is in closer agreement to the studies of Reinfried et al. (2009) and Bouet et al. (2012-)
396 who used COSMO-MUSCAT and RAMS-DPM respectively. Considering each study used a different model and
397 therefore physics, it is unsurprising that the results vary. However, it is not apparent how much of a role the region
398 or specific case study plays in this difference and is an area for future work.

399 The temporal trends in vertically integrated dust mass lag behind those observed in the DUP plots in Fig. 4.
400 Particularly at timesteps where DUP decreases, the change in integrated dust mass follows several hours later. The
401 time series of gravitational settling rates at the surface (Fig. 5.b) also lags behind the DUP trends, which implies that
402 the removal mechanisms for dust take time to act on the airborne particles once they are emitted. The rates of
403 gravitational settling are higher in the explicitconvection-permitting simulation compared to the coarse simulations,
404 yet because more dust is available aloft to settle out. Nevertheless, Fig. 6.a suggests that this increase in gravitational
405 settling rates in the 3 km case is not enough to offset the higher dust emissions, or the vertically integrated dust
406 quantities would be similar across all the simulations. The fact that the vertically integrated dust values are higher in
407 the 3 km simulation, despite higher rates of gravitational settling, implies there must be a mechanism that acts to
408 keep dust suspended longer in the explicitconvection-permitting simulations than in those with parameterized

409 convection. There are clearly more processes occurring above the surface to influence the vertically integrated dust
410 quantities than just a simple surface emission to surface deposition ratio. This will be further deconstructed by
411 examining vertical profiles in the following section.

412 3.2) Vertical characteristics

413 3.2.1) Vertical dust and velocity profiles

414 Moving away from vertically integrated quantities to a time and domain averaged vertical snapshot of dust (Fig.
415 7.a), the vertical dust profile follows a generally exponentially decreasing function and tapers off to low dust
416 concentrations in the range of 5-6 km above ground level (AGL). A widespread subsidence inversion is present near
417 6 km throughout the case study time period over the inner basin of the Arabian Peninsula (Fig 2), acting as a cap on
418 vertical motions and dust transport. Because dust concentrations do not vary much above this height, the plots in
419 Fig. 7 have been truncated at 9 km. There is a higher concentration of dust at every level in the explicitconvection-
420 allowing simulation compared to that in the coarse simulations. Examining the percent difference plot between the
421 explicitconvection-permitting and other simulations in Fig. 7.b, there is a difference of approximately 80% at the
422 surface, which increases upwards to ~180% at 6 km. Above this level, the percent difference between the
423 explicitconvection-permitting and coarse simulations changes sign, but the overall concentration is extremely low,
424 and as such, the authors make no attempt to assign meaning to the differences above 6 km.

425 For dust to reach higher levels in the atmosphere, it must have undergone vertical transport to move it aloft from its
426 initial source region at the surface. Several mechanisms could be responsible for vertical dust transport in the
427 Arabian Peninsula, including flow over terrain, daytime mixing (dry convection), and lastly, moist convective
428 updrafts, whose representation (explicit versus parameterized) is a defining difference between the horizontal
429 resolutions tested in this paper. Investigating the effect that increasing resolution has on updraft and downdraft
430 strength can be found in Fig. 8, which represents the mean of all vertical velocities above or below 0 m s^{-1} , including
431 points that are not vertically continuous. As resolution increases, the average range in vertical velocity also
432 increases. The simulations with parametrized convection have lower mean updraft / downdraft speeds than the
433 explicitconvection-allowing simulation, on the order ~75% weaker near the surface for the 15 km runs and ~110%
434 weaker for the 45 km run. It is known that in numerical models, the updraft radius scales with the grid spacing (e.g.
435 Bryan and Morrison, 2012), with a compensating increase in updraft speed as the radius decreases. This relationship
436 skews the frequency of vertical velocities to higher values. Irrespective of resolution, the mean updraft speeds in the
437 WRF-Chem simulations are slightly higher than the downdraft speeds ~~near the surface~~, while at the surface mean
438 downdraft speeds are higher than updraft speeds, a consideration that will be discussed further in Sect. 3.2.2.

439 3.2.2) Vertical dust flux

440 The implicationsimplication for dust transport based on vertical velocities is convoluted, since updrafts and
441 downdrafts work concurrently to redistribute aerosol. As noted in Jung et al. (2005), convective updrafts will lift
442 aerosol particles upward into the free atmosphere, while downdrafts simultaneously limit the maximum vertical

443 extent of these particles. However, the convective transport simulations in Jung et al. (2005) demonstrate that these
444 opposing processes do not act as equal opposites in time, magnitude, and space. This canon holds true for the
445 Arabian Peninsula simulations as well. Fig. 9 contains Contoured Frequency by Altitude Diagrams (CFADs) of
446 vertical velocity (Yuter and Houze, 1995) normalized by the total number of grid points in each simulation. The
447 normalization is performed to remove an artificial larger frequency in the higher resolution simulations that arises
448 because there are more grid spaces available to count. Because no vertical velocity threshold is imposed, a majority
449 of points straddle zero. To highlight variability away from the zero line, the CFAD contours are plotted on a log
450 scale.

451 Similar to the mean plots in Fig. 8, as resolution increases, so does the variability in updraft and downdraft speeds.
452 There is a striking difference between the spread in vertical velocities at all altitudes across the 45 km, 15 km mean,
453 and 3 km simulations in Fig. 9. In the 45 km run, most of the velocities straddle $\pm 1-2 \text{ m s}^{-1}$, whereas the
454 explicitconvection-permitting simulation ranges from -10 to 30 m s^{-1} . Not only is the range larger, but the
455 normalized frequency is greater in the fine resolution simulation as well. The inference here is that stronger updrafts
456 will transport dust higher in the atmosphere, and that stronger updrafts are observed more frequently in the
457 explicitconvection-allowing simulation, thereby enhancing the integratedvertical dust transport.

458 Combining the information on the vertical distribution of dust and updraft / downdraft speeds, it is possible to
459 calculate a domain averaged dust flux profile (Fig. 8). Again, the magnitude of the dust flux upwards and
460 downwards from the surface through 6 km AGL is higher in the explicitconvection-allowing simulation compared to
461 the parametrized simulations. Moreover, the mean near-surface upwards dust flux is stronger than that for the
462 downward dust flux, which coincides with the mean updraft speeds being slightly higher than the mean downdraft
463 speeds at these same vertical levels (Fig. 8). This relationship also holds in the dust flux CFADs (Fig. 9), in which
464 the upward and downward flux of dust has more variability in the 3 km simulation, and stronger vertical dust fluxes
465 are more frequent.

466 Similarly, there is more dust transport evident at higher vertical levels in the explicitconvection-permitting
467 simulation, which has implications for the residence time of the dust particles. As dust is transported higher in the
468 atmosphere, absent any sort of external motion or coagulation outside of gravitational settling, the atmospheric
469 lifetime of the particles will increase. Figure 10 shows the theoretical terminal velocity of dust particles in WRF-
470 Chem using the Stokes settling velocity with slip correction for pressure dependence (Fig. 10.a) and their lifetime
471 based on different starting heights in the atmosphere (Fig. 10.b), which increases exponentially away from the
472 surface. As such, dust in the explicitconvection-permitting simulation will take longer to settle out, leading to the
473 higher observed vertically integrated dust values (Fig. 5) compared to the parameterized simulations. Looking at the
474 distribution of downdrafts in the vertical velocity CFADs (Fig. 9), there is a clear bimodal signal aloft in both the
475 explicitconvection-permitting and 15 km simulations, being representative of two distinct subsidence layers, which
476 act as a cap on vertical transport. The local minimum occurs around 6 km, which could explain why dust fluxes also
477 taper off at this level.

478 At the surface, higher dust flux values are found in association with the downdrafts, producing a pronounced
479 skewness towards high, yet infrequent values of strong negative dust flux towards the ground (Fig. 9). It is
480 hypothesized that this skewness is a consequence of the dissimilar background dust conditions in the vicinity of
481 near-surface downdrafts and updrafts, similar to the results found in Siegel and van den Heever (2012), which
482 studied the ingestion of dust by a supercell storm. Updrafts originate in relatively clear air, and will consume
483 background dust and transport it upwards. However, downdrafts occur through the cold pool, and hence their source
484 is, at least partially, within the dusty cold pool. As such, downdrafts will have access to more dust and thus transport
485 more of it in the downward direction. This skewness warrants further research, preferably from an idealized
486 perspective, to better understand the relationship between storm dynamics, dust emissions, and transport.

487 In all, the increased vertical dust concentration profile and vertically integrated dust ~~concentrations~~values in the 3
488 km run are a product of several processes working together. Compared to the simulations with parameterized
489 convection, the 3 km run has enhanced potential for dust uplift due to stronger resolved downdrafts and lower wind
490 velocity thresholds, higher vertical transport due to more frequent, stronger updrafts, and a lengthier theoretical
491 residence time once being lofted to higher levels.

492 3.3) Impacts on radiation

493 Beyond the first-order sensitivity of model resolution to dust emissions and concentrations for the Arabian Peninsula
494 case study, there are higher-order effects that disseminate from changing dust concentrations. One example being
495 the modification of atmospheric heating / cooling rates and the radiation budget due to dust absorption and scattering
496 (see Sect. 1). The domain and time averaged shortwave (SW), longwave (LW), and net dust heating / cooling rates
497 are found in Fig. 11. The average dust heating and cooling rates were calculated over the last 48 hours of the
498 simulation as a difference between the radiation tendency with dust aerosols and without. Ostensibly, since dust
499 concentrations increase in the model as resolution increases, so does the magnitude of the radiative effects. There is
500 a stronger SW cooling and LW heating effect in the 3 km simulation, and this trend follows the vertical distribution
501 of dust from Fig. 7, again tapering off near 5-6 km AGL.

502 Most interestingly, however, is the difference in the net aerosol heating rate. In the lowest layer (<1.5 km), there is a
503 sign change between the fine and coarse simulations. The SW effect in the explicit convection-allowing simulation is
504 strong enough to elicit a net cooling effect in this near-surface layer. Conversely, the LW aerosol heating effect
505 dominates in the coarse simulations, resulting in a net warming effect. The model has a stronger shortwave effect for
506 dust based on the prescribed index of refraction, but is also related to the timing of dust emissions, considering the
507 SW effect is only active during the daytime. The difference between warming and cooling can have cascading
508 effects on the thermodynamic profile, static stability, and future convective development, which in turn impacts the
509 relative importance between convection and the NLLJ discussed earlier. The sensitivity of dust concentrations to
510 horizontal model resolution is important to understand in its own right, but furthermore, this sensitivity leads to
511 higher-order changes in model predictions. If NWP models or GCMs are going to incorporate dust radiative effects,

512 concentrations need to be highly constrained, not only to accurately capture the magnitude, but the sign of the
513 response as well.

514

515 **4) Discussion and recommendations**

516 For this Arabian Peninsula event, horizontal resolution in the WRF-Chem model has a considerable effect on the
517 dust budget of the region. Because aerosol prediction models and GCMs still employ cumulus parameterizations, it
518 is important to discuss the uncertainties unearthed in this paper, as well as recommendations for past and future
519 forecasts and research that will be generated prior to our ability to consistently run these models at convection-
520 permitting resolutions.

521 In an average sense, there will be higher dust concentrations produced in ~~explicit~~-convection-permitting simulations
522 compared to those with parameterized convection. The major point here is that the uncertainty in dust concentrations
523 for simulations using different cumulus parameterizations (15 km ensemble), or using different horizontal
524 resolutions with the same cumulus parameterizations (45 km versus 15 km) is small relative to the differences
525 between the use of parameterized versus ~~explicit~~-convection-allowing scales. *Most of the uncertainty in the model's*
526 *predicted dust concentrations comes from the choice to either parameterize ~~or explicitly resolve~~-convection-or run*
527 *at convection-permitting scales.*

528 The results of this research do not stand alone in the literature focused on the impact of horizontal model resolution
529 on dust emissions, and there are several similarities and differences to note when comparing this paper to previous
530 studies. Firstly, concerning the diurnal variation in dust emissions, we find a similar response in the NLLJ
531 mechanism to that of Heinhold et al. (2013) and Marsham et al. (2011), whereby the coarsest simulations
532 overestimate the early morning windspeeds caused by the mixing of the jet to the surface and fail to capture the late
533 afternoon / early evening convective dust lofting mechanism. In these previous studies, the ~~explicitconvection-~~
534 allowing simulation reduces the importance of the NLLJ and enhances the convective maximum, but still retains the
535 NLLJ as the dominant process for dust uplift. Overall, Heinhold et al. (2013) and Marsham et al. (2011) found a net
536 reduction in dust uplift ~~with explicit~~while running at convection-permitting scales. While the NLLJ mechanism is
537 found to be similar here, the analysis reveals an opposite response in WRF-Chem for the Arabian Peninsula, in
538 which the convective maximum dominates, but the NLLJ is still an important mechanism, which thereby leads to
539 more, rather than less dust in the ~~explicitconvection-~~allowing simulations. The net increase in dust concentrations in
540 WRF-Chem is similar to the findings of Reinfried et al. (2009), although Reinfried et al. (2009) focused mainly on
541 haboobs, which may point to convection being the source of agreement rather than the balance between the NLLJ
542 and convection. At this point, we cannot determine whether the discrepancies between our results and previous
543 literature comes from regional or case study differences in the importance of these mechanisms to the dust budget,
544 differences in the models' representation of these processes, or a combination of the two. In all, more work needs to

545 be done to investigate the relationship between the NLLJ and subsequent late afternoon convection in dust
546 producing regions, and the representation of this in numerical models.

547 From ~~an~~ vertically integrated viewpoint, for the Arabian Peninsula region it is possible to rudimentarily tune the
548 dust concentrations of the coarse simulations to that of the ~~explicit~~convection-permitting simulation by multiplying
549 by an average constant derived from the dust difference plots in Fig. 6-7, which would be on the order of ~ 2 . This is
550 an offline solution, which would aid in enhancing the accuracy of a first-order forecast of vertically integrated or
551 surface dust, and/or AOD. Nevertheless, attempting to use this tuning parameter online in the model (i.e. adjusting
552 the tuning constant, C , in Eq. 1) would not reconcile the differences from a dust flux standpoint. Even if more dust
553 were to be emitted from the surface, the parameterized simulations still lack the necessary variability in updrafts and
554 downdrafts, especially updraft strength, to transport the dust upwards and away from the surface, thus
555 misrepresenting the atmospheric lifetime of these particles in the process.

556 Moreover, tuning the dust concentrations will not change the effect horizontal resolution has on the soil
557 characteristics, particularly soil moisture, and hence on the a priori determined threshold wind speeds which are
558 important in calculating dust lofting in the first place (Fig. 4). If dust concentrations are inaccurately predicted in the
559 coarse simulations, or erroneously tuned, the higher-order online feedbacks will also be incorrect, such as
560 modifications to the radiative budget, and feedbacks to the thermodynamic profile, static stability and mesoscale
561 features, particularly those driven by differences in thermodynamic gradients, such as sea breezes and cold pool
562 propagation.

563 **5) Conclusions**

564 In this study, we have quantified the response sign and magnitude in modeled dust fields in the WRF-Chem regional
565 model to increasing horizontal resolution and the manner in which convection is represented for a summertime
566 Arabian Peninsula event. We have investigated the variability in dust concentrations and fluxes due to the choice of
567 convective parameterization, the representation of convection in the model (explicit versus parameterized), and the
568 effect these differences in dust concentrations have on aerosol heating rates. The case study was simulated at three
569 different horizontal resolutions (45 km, 15 km, and 3 km), with the two coarsest simulations run with cumulus
570 parameterizations, and the 3 km simulation run at convection-permitting resolution. To understand the uncertainty
571 across different parameterizations, five separate cumulus parameterizations were tested in an ensemble (BMJ, AS,
572 GD, TD, KF) at 15 km grid spacing.

573 The ~~explicit~~convection-allowing simulation exhibited a stronger potential for dust uplift as a function of modeled
574 wind speed, wind threshold, and the location of dust sources. The wind threshold for dust lofting in the 3 km
575 simulation was on average, lower than that for the 15 km or 45 km. This is due to differences in grid resolution
576 leading to changes in the soil moisture, whereby the 3 km simulation displays lower soil wetness across the domain.
577 Furthermore, a distinct difference across simulations was identified in the representation of the bimodal daily
578 maximum in dust emissions in the local mid-morning (mixing of the NLLJ to the surface) and late afternoon

579 (convective outflow boundaries). Compared to the 3 km case, the 45 km simulation overestimates the contribution
580 from the NLLJ and underestimates the role of convection in dust emissions.

581 The 3 km simulation also produced higher vertically integrated dust values at every timestep, as well as higher dust
582 concentrations at every vertical level in the lower troposphere (below 6 km AGL). The uncertainty in dust
583 concentrations for simulations using different cumulus parameterizations (15 km ensemble spread) is much smaller
584 than the difference between the parameterized and explicitconvection-permitting convection cases. For the WRF-
585 Chem Arabian Peninsula simulations, the modeled dust fields were most sensitive to the choice of parametrizing or
586 explicitly resolving convective processes. The enhanced dust concentrations in the explicitconvection-allowing case
587 are the result of stronger downdrafts lofting more dust from the surface, and stronger updrafts carrying dust to higher
588 levels of the atmosphere, thereby increasing the airborne lifetime of the dust particles. The difference in dust mass
589 across the simulations leads to a significant modification of the radiation budget, specifically the aerosol heating
590 rate. The explicitconvection-allowing simulation revealed a greater shortwave and longwave effect, and for aerosol
591 heating rates in the lowest levels, shortwave cooling is stronger than longwave heating, leading to a net cooling
592 effect. Conversely, the opposite radiative response is present in the parameterized cases, resulting in a net warming
593 effect, causing a change in sign in the lowest levels compared to the explicitconvection-permitting case.

594 There are a number of implications these results may have on forecasting and future studies. The dust concentrations
595 in the coarse simulations could be tuned offline to match those in the explicitconvection-allowing simulation using
596 the percentage difference plots included in Fig. 5-6. This tuning would be on the order of ~2. However, because
597 vertical transport is essential to the vertical concentrations and lifetime of the particles, this tuning factor cannot be
598 applied online. Even if such a tuning were applied, this change will not accurately capture higher-order feedbacks to
599 the meteorology, thermodynamic environment and radiation budget of the Arabian Peninsula, or to the soil moisture
600 wind threshold velocities. Finally, this work also points to the need to better constrain dust concentrations in
601 numerical models, and further develop our understanding of the relationship between storm dynamics and dust
602 processes.

603 **Author contributions**

604 Jennie Bukowski (JB) and Susan C. van den Heever (SvdH) designed the experiments. JB set up and performed the
605 WRF-Chem simulations and wrote the analysis code. Both JB and SvdH contributed to the analysis of the model
606 output. JB prepared the manuscript with contributions and edits from SvdH.

607 **Competing interests**

608 The authors declare that they have no conflict of interest.

609 **Acknowledgements**

610 This work was funded by an Office of Naval Research – Multidisciplinary University Research Initiative (ONR-
611 MURI) grant (# N00014-16-1-2040). Jennie Bukowski was partially supported by the Cooperative Institute for
612 Research in the Atmosphere (CIRA) Program of Research and Scholarly Excellence (PRSE) fellowship. The
613 simulation data are available upon request from the corresponding author, Jennie Bukowski. Initialization data for
614 the model was provided by: National Centers for Environmental Prediction, National Weather Service, NOAA, U.S.
615 Department of Commerce. 2000, updated daily. NCEP FNL Operational Model Global Tropospheric Analyses,
616 continuing from July 1999. Research Data Archive at the National Center for Atmospheric Research, Computational
617 and Informational Systems Laboratory. <https://doi.org/10.5065/D6M043C6>.

618 **References**

- 619 [Alizadeh Choobari, O., Zawar-Reza, P., and Sturman, A.: Low level jet intensification by mineral dust aerosols,](#)
620 [Ann. Geophys., 31, 625–632, doi:10.5194/angeo-31-625-2013, 2013.](#)
- 621 Almazroui, M.: Calibration of TRMM rainfall climatology over Saudi Arabia during 1998–2009, *Atmos. Res.*,
622 99(3–4), 400–414, doi:10.1016/J.ATMOSRES.2010.11.006, 2011.
- 623 Aoki, T., Tanaka, T. Y., Uchiyama, A., Chiba, M., Mikami, M., Yabuki, S. And Key, J. R.: Sensitivity Experiments
624 of Direct Radiative Forcing Caused by Mineral Dust Simulated with a Chemical Transport Model, *J.*
625 *Meteorol. Soc. Japan. Ser. II*, 83A, 315–331, doi:10.2151/jmsj.83A.315, 2005.
- 626 Arakawa, A. and Schubert, W. H.: Interaction of a Cumulus Cloud Ensemble with the Large-Scale Environment,
627 Part I, *J. Atmos. Sci.*, 31(3), 674–701, doi:10.1175/1520-0469(1974)031<0674:IOACCE>2.0.CO;2, 1974.
- 628 Babu, C. A., Jayakrishnan, P. R. and Varikoden, H.: Characteristics of precipitation pattern in the Arabian Peninsula
629 and its variability associated with ENSO, *Arab. J. Geosci.*, 9(3), 186, doi:10.1007/s12517-015-2265-x,
630 2016.
- 631 Baddock, M. C., Strong, C. L., Leys, J. F., Heidenreich, S. K., Tews, E. K. and McTainsh, G. H.: A visibility and
632 total suspended dust relationship, *Atmos. Environ.*, 89, 329–336, doi:10.1016/J.ATMOSENV.2014.02.038,
633 2014.
- 634 Barnard, J. C., Fast, J. D., Paredes-Miranda, G., Arnott, W. P. and Laskin, A.: Technical Note: Evaluation of the
635 WRF-Chem “Aerosol Chemical to Aerosol Optical Properties Module” using data from the MILAGRO
636 campaign, *Atmos. Chem. Phys.*, 10(15), 7325–7340, doi:10.5194/acp-10-7325-2010, 2010.
- 637 Beegum, S. N., Gherboudj, I., Chaouch, N., Temimi, M. and Ghedira, H.: Simulation and analysis of synoptic scale
638 dust storms over the Arabian Peninsula, *Atmos. Res.*, 199, 62–81, doi:10.1016/J.ATMOSRES.2017.09.003,
639 2018.
- 640 Benedetti, A., Reid, J. S., Knippertz, P., Marsham, J. H., Di Giuseppe, F., Rémy, S., Basart, S., Boucher, O., Brooks,
641 I. M., Menut, L., Mona, L., Laj, P., Pappalardo, G., Wiedensohler, A., Baklanov, A., Brooks, M., Colarco,
642 P. R., Cuevas, E., da Silva, A., Escribano, J., Flemming, J., Huneus, N., Jorba, O., Kazadzis, S., Kinne, S.,
643 Popp, T., Quinn, P. K., Sekiyama, T. T., Tanaka, T. and Terradellas, E.: Status and future of numerical
644 atmospheric aerosol prediction with a focus on data requirements, *Atmos. Chem. Phys.*, 18(14), 10615–
645 10643, doi:10.5194/acp-18-10615-2018, 2018.

646 Benedetti, A., Baldasano, J. M., Basart, S., Benincasa, F., Boucher, O., Brooks, M. E., Chen, J.-P., Colarco, P. R.,
647 Gong, S., Huneeus, N., Jones, L., Lu, S., Menut, L., Morcrette, J.-J., Mulcahy, J., Nickovic, S., Pérez
648 García-Pando, C., Reid, J. S., Sekiyama, T. T., Tanaka, T. Y., Terradellas, E., Westphal, D. L., Zhang, X.-
649 Y. and Zhou, C.-H.: Operational Dust Prediction, in *Mineral Dust: A Key Player in the Earth System*,
650 edited by P. Knippertz and J.-B. W. Stuut, pp. 223–265, Springer Netherlands, Dordrecht., 2014.

651 Benedetti, A., Reid, J. S. and Colarco, P. R.: International Cooperative for Aerosol Prediction Workshop on Aerosol
652 Forecast Verification, *Bull. Am. Meteorol. Soc.*, 92(11), ES48-ES53, doi:10.1175/BAMS-D-11-00105.1,
653 2011.

654 Bishop, J. K. B., Davis, R. E. and Sherman, J. T.: Robotic Observations of Dust Storm Enhancement of Carbon
655 Biomass in the North Pacific, *Science* (80-.), 298(5594), 817 LP-821, doi:10.1126/science.1074961, 2002.

656 Boose, Y., Welti, A., Atkinson, J., Ramelli, F., Danielczok, A., Bingemer, H. G., Plötze, M., Sierau, B., Kanji, Z. A.
657 and Lohmann, U.: Heterogeneous ice nucleation on dust particles sourced from nine~deserts worldwide --
658 Part 1: Immersion freezing, *Atmos. Chem. Phys.*, 16(23), 15075–15095, doi:10.5194/acp-16-15075-2016,
659 2016.

660 Bouet, C., Cautenet, G., Bergametti, G., Marticorena, B., Todd, M. C. and Washington, R.: Sensitivity of desert dust
661 emissions to model horizontal grid spacing during the Bodélé Dust Experiment 2005, *Atmos. Environ.*, 50,
662 377–380, doi:10.1016/J.ATMOSENV.2011.12.037, 2012.

663 [Bryan, G. H. and Morrison, H.: Sensitivity of a Simulated Squall Line to Horizontal Resolution and](#)
664 [Parameterization of Microphysics, *MWR*, 140, 202-225, doi:10.1175/MWR-D-11-00046.1, 2012.](#)

665 Camino, C., Cuevas, E., Basart, S., Alonso-Pérez, S., Baldasano, J. M., Terradellas, E., Marticorena, B., Rodríguez,
666 S. and Berjón, A.: An empirical equation to estimate mineral dust concentrations from visibility
667 observations in Northern Africa, *Aeolian Res.*, 16, 55–68, doi:10.1016/J.AEOLIA.2014.11.002, 2015.

668 Chou, M.-D. and Suarez, M. J.: Technical Report Series on Global Modeling and Data Assimilation A Thermal
669 Infrared Radiation Parameterization for Atmospheric Studies Revised May 2003, Nasa Tech. Memo. 15,
670 NASA, 40 pp., 1999.

671 Corr, C. A., Ziemba, L. D., Scheuer, E., Anderson, B. E., Beyersdorf, A. J., Chen, G., Crosbie, E., Moore, R. H.,
672 Shook, M., Thornhill, K. L., Winstead, E., Lawson, R. P., Barth, M. C., Schroeder, J. R., Blake, D. R. and
673 Dibb, J. E.: Observational evidence for the convective transport of dust over the Central United States, *J.*
674 *Geophys. Res. Atmos.*, 121(3), 1306–1319, doi:10.1002/2015JD023789, 2016.

675 Cowie, S. M., Marsham, J. H. and Knippertz, P.: The importance of rare, high-wind events for dust uplift in northern
676 Africa, *Geophys. Res. Lett.*, 42(19), 8208–8215, doi:10.1002/2015GL065819, 2015.

677 Dayan, U., Ziv, B., Margalit, A., Morin, E. and Sharon, D.: A severe autumn storm over the middle-east: synoptic
678 and mesoscale convection analysis, *Theor. Appl. Climatol.*, 69(1), 103–122, doi:10.1007/s007040170038,
679 2001.

680 Dipu, S., Prabha, T. V., Pandithurai, G., Dudhia, J., Pfister, G., Rajesh, K. and Goswami, B. N.: Impact of elevated
681 aerosol layer on the cloud macrophysical properties prior to monsoon onset, *Atmos. Environ.*, 70, 454–467,
682 doi:10.1016/J.ATMOSENV.2012.12.036, 2013.

683 Fadnavis, S., Semeniuk, K., Pozzoli, L., Schultz, M. G., Ghude, S. D., Das, S. and Kakatkar, R.: Transport of
684 aerosols into the UTLS and their impact on the Asian monsoon region as seen in a global model simulation,
685 *Atmos. Chem. Phys.*, 13(17), 8771–8786, doi:10.5194/acp-13-8771-2013, 2013.

686 Fast, J. D., Gustafson Jr., W. I., Easter, R. C., Zaveri, R. A., Barnard, J. C., Chapman, E. G., Grell, G. A. and
687 Peckham, S. E.: Evolution of ozone, particulates, and aerosol direct radiative forcing in the vicinity of
688 Houston using a fully coupled meteorology-chemistry-aerosol model, *J. Geophys. Res. Atmos.*, 111(D21),
689 doi:10.1029/2005JD006721, 2006.

690 Field, P. R., Möhler, O., Connolly, P., Krämer, M., Cotton, R., Heymsfield, A. J., Saathoff, H. and Schnaiter, M.:
691 Some ice nucleation characteristics of Asian and Saharan desert dust, *Atmos. Chem. Phys.*, 6(10), 2991–
692 3006, doi:10.5194/acp-6-2991-2006, 2006.

693 Giannakopoulou, E. M. and Toumi, R.: The Persian Gulf summertime low-level jet over sloping terrain, *Q. J. R.*
694 *Meteorol. Soc.*, 138(662), 145–157, doi:10.1002/qj.901, 2012.

695 Ginoux, P., Chin, M., Tegen, I., Prospero, J. M., Holben, B., Dubovik, O. and Lin, S.-J.: Sources and distributions of
696 dust aerosols simulated with the GOCART model, *J. Geophys. Res. Atmos.*, 106(D17), 20255–20273,
697 doi:10.1029/2000JD000053, 2001.

698 Ginoux, P., Prospero, J. M., Gill, T. E., Hsu, N. C. and Zhao, M.: Global-scale attribution of anthropogenic and
699 natural dust sources and their emission rates based on MODIS Deep Blue aerosol products, *Rev. Geophys.*,
700 50(3), doi:10.1029/2012RG000388, 2012.

701 Grell, G. A., Peckham, S. E., Schmitz, R., McKeen, S. A., Frost, G., Skamarock, W. C. and Eder, B.: Fully coupled
702 “online” chemistry within the WRF model, *Atmos. Environ.*, 39(37), 6957–6975,
703 doi:10.1016/J.ATMOSENV.2005.04.027, 2005.

704 Hasanean, H., Almazroui, M., Hasanean, H. and Almazroui, M.: Rainfall: Features and Variations over Saudi
705 Arabia, *A Review, Climate*, 3(3), 578–626, doi:10.3390/cli3030578, 2015.

706 Haywood, J. M., Allan, R. P., Culverwell, I., Slingo, T., Milton, S., Edwards, J. and Clerbaux, N.: Can desert dust
707 explain the outgoing longwave radiation anomaly over the Sahara during July 2003?, *J. Geophys. Res.*
708 *Atmos.*, 110(D5), doi:10.1029/2004JD005232, 2005.

709 Heald, C. L., Ridley, D. A., Kroll, J. H., Barrett, S. R. H., Cady-Pereira, K. E., Alvarado, M. J. and Holmes, C. D.:
710 Contrasting the direct radiative effect and direct radiative forcing of aerosols, *Atmos. Chem. Phys.*, 14(11),
711 5513–5527, doi:10.5194/acp-14-5513-2014, 2014.

712 Heinold, B., Knippertz, P., Marsham, J. H., Fiedler, S., Dixon, N. S., Schepanski, K., Laurent, B. and Tegen, I.: The
713 role of deep convection and nocturnal low-level jets for dust emission in summertime West Africa:
714 Estimates from convection-permitting simulations, *J. Geophys. Res. Atmos.*, 118(10), 4385–4400,
715 doi:10.1002/jgrd.50402, 2013.

716 Huneeus, N., Schulz, M., Balkanski, Y., Griesfeller, J., Prospero, J., Kinne, S., Bauer, S., Boucher, O., Chin, M.,
717 Dentener, F., Diehl, T., Easter, R., Fillmore, D., Ghan, S., Ginoux, P., Grini, A., Horowitz, L., Koch, D.,
718 Krol, M. C., Landing, W., Liu, X., Mahowald, N., Miller, R., Morcrette, J.-J., Myhre, G., Penner, J.,

719 Perlwitz, J., Stier, P., Takemura, T. and Zender, C. S.: Global dust model intercomparison in AeroCom
720 phase I, *Atmos. Chem. Phys.*, 11(15), 7781–7816, doi:10.5194/acp-11-7781-2011, 2011.

721 Jickells, T. and Moore, C. M.: The Importance of Atmospheric Deposition for Ocean Productivity, *Annu. Rev. Ecol.*
722 *Evol. Syst.*, 46(1), 481–501, doi:10.1146/annurev-ecolsys-112414-054118, 2015.

723 Jish Prakash, P., Stenchikov, G., Kalenderski, S., Osipov, S. and Bangalath, H.: The impact of dust storms on the
724 Arabian Peninsula and the Red Sea, *Atmos. Chem. Phys.*, 15(1), 199–222, doi:10.5194/acp-15-199-2015,
725 2015.

726 Jung, E., Shao, Y. and Sakai, T.: A study on the effects of convective transport on regional-scale Asian dust storms
727 in 2002, *J. Geophys. Res. Atmos.*, 110(D20), doi:10.1029/2005JD005808, 2005.

728 Kain, J. S.: The Kain–Fritsch Convective Parameterization: An Update, *J. Appl. Meteorol.*, 43(1), 170–181,
729 doi:10.1175/1520-0450(2004)043<0170:TKCPAU>2.0.CO;2, 2004.

730 Kalenderski, S., Stenchikov, G. and Zhao, C.: Modeling a typical winter-time dust event over the Arabian Peninsula
731 and the Red Sea, *Atmos. Chem. Phys.*, 13(4), 1999–2014, doi:10.5194/acp-13-1999-2013, 2013.

732 Kalenderski, S. and Stenchikov, G.: High-resolution regional modeling of summertime transport and impact of
733 African dust over the Red Sea and Arabian Peninsula, *J. Geophys. Res. Atmos.*, 121(11), 6435–6458,
734 doi:10.1002/2015JD024480, 2016.

735 Karydis, V. A., Kumar, P., Barahona, D., Sokolik, I. N. and Nenes, A.: On the effect of dust particles on global
736 cloud condensation nuclei and cloud droplet number, *J. Geophys. Res. Atmos.*, 116(D23),
737 doi:10.1029/2011JD016283, 2011.

738 Kinne, S., Lohmann, U., Feichter, J., Schulz, M., Timmreck, C., Ghan, S., Easter, R., Chin, M., Ginoux, P.,
739 Takemura, T., Tegen, I., Koch, D., Herzog, M., Penner, J., Pitari, G., Holben, B., Eck, T., Smirnov, A.,
740 Dubovik, O., Slutsker, I., Tanre, D., Torres, O., Mishchenko, M., Geogdzhayev, I., Chu, D. A. and
741 Kaufman, Y.: Monthly averages of aerosol properties: A global comparison among models, satellite data,
742 and AERONET ground data, *J. Geophys. Res. Atmos.*, 108(D20), doi:10.1029/2001JD001253, 2003.

743 Kishcha, P., Alpert, P., Barkan, J., Kirschner, I. and Machenhauer, B.: Atmospheric response to Saharan dust
744 deduced from ECMWF reanalysis (ERA) temperature increments, *Tellus B Chem. Phys. Meteorol.*, 55(4),
745 901–913, doi:10.3402/tellusb.v55i4.16380, 2011.

746 Klich, C. A. and Fuelberg, H. E.: The role of horizontal model resolution in assessing the transport of CO in a
747 middle latitude cyclone using WRF-Chem, *Atmos. Chem. Phys.*, 14(2), 609–627, doi:10.5194/acp-14-609-
748 2014, 2014.

749 [Klose, M. and Shao, Y.: Stochastic parameterization of dust emission and application to convective atmospheric](#)
750 [conditions, *Atmos. Chem. Phys.*, 12, 7309-7320, doi:10.5194/acp-12-7309-2012, 2012.](#)

751 Knopf, D. A. and Koop, T.: Heterogeneous nucleation of ice on surrogates of mineral dust, *J. Geophys. Res. Atmos.*,
752 111(D12), doi:10.1029/2005JD006894, 2006.

753 Kok, J. F., Mahowald, N. M., Fratini, G., Gillies, J. A., Ishizuka, M., Leys, J. F., Mikami, M., Park, M.-S., Park, S.-

754 U., Van Pelt, R. S. and Zobeck, T. M.: An improved dust emission model – Part 1: Model description and
755 comparison against measurements, *Atmos. Chem. Phys.*, 14(23), 13023–13041, doi:10.5194/acp-14-13023-
756 2014, 2014.

757 Kok, J. F., Ward, D. S., Mahowald, N. M. and Evan, A. T.: Global and regional importance of the direct dust-
758 climate feedback, *Nat. Commun.*, 9(1), 241, doi:10.1038/s41467-017-02620-y, 2018.

759 Largeron, Y., Guichard, F., Bouniol, D., Couvreux, F., Kergoat, L. and Marticorena, B.: Can we use surface wind
760 fields from meteorological reanalyses for Sahelian dust emission simulations?, *Geophys. Res. Lett.*, 42(7),
761 2490–2499, doi:10.1002/2014GL062938, 2015.

762 Lee, Y. H., Chen, K. and Adams, P. J.: Development of a global model of mineral dust aerosol microphysics,
763 *Atmos. Chem. Phys.*, 9(7), 2441–2458, doi:10.5194/acp-9-2441-2009, 2009.

764 Liao, H. and Seinfeld, J. H.: Radiative forcing by mineral dust aerosols: Sensitivity to key variables, *J. Geophys.*
765 *Res. Atmos.*, 103(D24), 31637–31645, doi:10.1029/1998JD200036, 1998.

766 Mahowald, N. M., Ballantine, J. A., Feddema, J. and Ramankutty, N.: Global trends in visibility: implications for
767 dust sources, *Atmos. Chem. Phys.*, 7(12), 3309–3339, doi:10.5194/acp-7-3309-2007, 2007.

768 Mahowald, N. M., Baker, A. R., Bergametti, G., Brooks, N., Duce, R. A., Jickells, T. D., Kubilay, N., Prospero, J.
769 M. and Tegen, I.: Atmospheric global dust cycle and iron inputs to the ocean, *Global Biogeochem. Cycles*,
770 19(4), doi:10.1029/2004GB002402, 2005.

771 Manktelow, P. T., Carslaw, K. S., Mann, G. W. and Spracklen, D. V.: The impact of dust on sulfate aerosol, CN and
772 CCN during an East Asian dust storm, *Atmos. Chem. Phys.*, 10(2), 365–382, doi:10.5194/acp-10-365-
773 2010, 2010.

774 Marsham, J. H., Parker, D. J., Grams, C. M., Taylor, C. M. and Haywood, J. M.: Uplift of Saharan dust south of the
775 intertropical discontinuity, *J. Geophys. Res. Atmos.*, 113(D21), doi:10.1029/2008JD009844, 2008.

776 Marsham, J. H., Knippertz, P., Dixon, N. S., Parker, D. J. and Lister, G. M. S.: The importance of the representation
777 of deep convection for modeled dust-generating winds over West Africa during summer, *Geophys. Res.*
778 *Lett.*, 38(16), doi:10.1029/2011GL048368, 2011.

779 Marticorena, B. and Bergametti, G.: Modeling the atmospheric dust cycle: 1. Design of a soil-derived dust emission
780 scheme, *J. Geophys. Res. Atmos.*, 100(D8), 16415–16430, doi:10.1029/95JD00690, 1995.

781 Martin, J. H.: Iron still comes from above, *Nature*, 353(6340), 123, doi:10.1038/353123b0, 1991.

782 Menut, L.: Sensitivity of hourly Saharan dust emissions to NCEP and ECMWF modeled wind speed, *J. Geophys.*
783 *Res. Atmos.*, 113(D16), doi:10.1029/2007JD009522, 2008.

784 Miller, S. D., [Grasso, L., Bian, Q., Kreidenweis, S., Dostalek, J., Solbrig, J., Bukowski, J., van den Heever, S. C.,](#)
785 [Wang, Y., Xu, X., Wang, J., Walker, A., Wu, T.-C., Zupanski, M., Chiu, C., and Reid, J.: *A Tale of Two*](#)
786 [Dust Storms: Analysis of a Complex Dust Event in the Middle East. *Atmos. Meas. Tech. Discuss.*,](#)
787 [doi:10.5194/amt-2019-82, 2019.](#)

788 [Miller, S. D.,](#) Kuciauskas, A. P., Liu, M., Ji, Q., Reid, J. S., Breed, D. W., Walker, A. L. and Mandoos, A. Al:
789 Haboob dust storms of the southern Arabian Peninsula, *J. Geophys. Res. Atmos.*, 113(D1),
790 doi:10.1029/2007JD008550, 2008.

791 Morrison, H., Curry, J. A. and Khvorostyanov, V. I.: A New Double-Moment Microphysics Parameterization for
792 Application in Cloud and Climate Models. Part I: Description, *J. Atmos. Sci.*, 62(6), 1665–1677,
793 doi:10.1175/JAS3446.1, 2005.

794 Morrison, H., Thompson, G. and Tatarskii, V.: Impact of Cloud Microphysics on the Development of Trailing
795 Stratiform Precipitation in a Simulated Squall Line: Comparison of One- and Two-Moment Schemes, *Mon.*
796 *Weather Rev.*, 137(3), 991–1007, doi:10.1175/2008MWR2556.1, 2009.

797 Nakanishi, M. and Niino, H.: An Improved Mellor–Yamada Level-3 Model: Its Numerical Stability and Application
798 to a Regional Prediction of Advection Fog, *Boundary-Layer Meteorol.*, 119(2), 397–407,
799 doi:10.1007/s10546-005-9030-8, 2006.

800 Nakanishi, M. and NIINO, H.: Development of an Improved Turbulence Closure Model for the Atmospheric
801 Boundary Layer, *J. Meteorol. Soc. Japan. Ser. II*, 87(5), 895–912, doi:10.2151/jmsj.87.895, 2009.

802 National Centers for Environmental Prediction/National Weather Service/NOAA/U.S. Department of Commerce:
803 NCEP GDAS/FNL 0.25 Degree Global Tropospheric Analyses and Forecast Grids, Research Data Archive
804 at the National Center for Atmospheric Research, Computational and Information Systems Laboratory,
805 Boulder, CO, <https://doi.org/10.5065/D65Q4T4Z>, 2015.

806 Niu, G.-Y., Yang, Z.-L., Mitchell, K. E., Chen, F., Ek, M. B., Barlage, M., Kumar, A., Manning, K., Niyogi, D.,
807 Rosero, E., Tewari, M. and Xia, Y.: The community Noah land surface model with multiparameterization
808 options (Noah-MP): 1. Model description and evaluation with local-scale measurements, *J. Geophys. Res.*
809 *Atmos.*, 116(D12), doi:10.1029/2010JD015139, 2011.

810 Pantillon, F., Knippertz, P., Marsham, J. H. and Birch, C. E.: A Parameterization of Convective Dust Storms for
811 Models with Mass-Flux Convection Schemes, *J. Atmos. Sci.*, 72(6), 2545–2561, doi:10.1175/JAS-D-14-
812 0341.1, 2015.

813 Pantillon, F., Knippertz, P., Marsham, J. H., Panitz, H.-J. and Bischoff-Gauss, I.: Modeling haboob dust storms in
814 large-scale weather and climate models, *J. Geophys. Res. Atmos.*, 121(5), 2090–2109,
815 doi:10.1002/2015JD024349, 2016.

816 Pérez, C., Nickovic, S., Pejanovic, G., Baldasano, J. M. and Özsoy, E.: Interactive dust-radiation modeling: A step
817 to improve weather forecasts, *J. Geophys. Res. Atmos.*, 111(D16), doi:10.1029/2005JD006717, 2006.

818 Pope, R. J., Marsham, J. H., Knippertz, P., Brooks, M. E. and Roberts, A. J.: Identifying errors in dust models from
819 data assimilation, *Geophys. Res. Lett.*, 43(17), 9270–9279, doi:10.1002/2016GL070621, 2016.

820 Prospero, J. M.: Long-term measurements of the transport of African mineral dust to the southeastern United States:
821 Implications for regional air quality, *J. Geophys. Res. Atmos.*, 104(D13), 15917–15927,
822 doi:10.1029/1999JD900072, 1999.

823 Reid, J. S., Benedetti, A., Colarco, P. R. and Hansen, J. A.: International Operational Aerosol Observability
824 Workshop, *Bull. Am. Meteorol. Soc.*, 92(6), ES21–ES24, doi:10.1175/2010BAMS3183.1, 2010.

825 Reinfried, F., Tegen, I., Heinold, B., Hellmuth, O., Schepanski, K., Cubasch, U., Huebener, H. and Knippertz, P.:

826 Simulations of convectively-driven density currents in the Atlas region using a regional model: Impacts on
827 dust emission and sensitivity to horizontal resolution and convection schemes, *J. Geophys. Res. Atmos.*,
828 114(D8), doi:10.1029/2008JD010844, 2009.

829 Ridley, D. A., Heald, C. L., Pierce, J. R. and Evans, M. J.: Toward resolution-independent dust emissions in global
830 models: Impacts on the seasonal and spatial distribution of dust, *Geophys. Res. Lett.*, 40(11), 2873–2877,
831 doi:10.1002/grl.50409, 2013.

832 Roberts, A. J., Woodage, M. J., Marsham, J. H., Highwood, E. J., Ryder, C. L., McGinty, W., Wilson, S., and
833 Crook, J.: Can explicit convection improve modelled dust in summertime West Africa?, *Atmos. Chem.*
834 *Phys.*, 18, 9025-9048, <https://doi.org/10.5194/acp-18-9025-2018>, 2018.

835 Saleeby, S. M., van den Heever, S. C., Bukowski, J., Walker, A. L., Solbrig, J. E., Atwood, S. A., Bian, Q.,
836 Kreidenweis, S. M., Wang, Y., Wang, J. and Miller, S. D.: The Influence of Simulated Surface Dust
837 Lofting Erodible Fraction on Radiative Forcing, *Atmos. Chem. Phys. Discuss.*, 2019, 1–35,
838 doi:10.5194/acp-2018-1302, 2019.

839 Schepanski, K., Knippertz, P., Fiedler, S., Timouk, F. and Demarty, J.: The sensitivity of nocturnal low-level jets
840 and near-surface winds over the Sahel to model resolution, initial conditions and boundary-layer set-up.
841 *Q.J.R. Meteorol. Soc.*, 141, 1442-1456. doi:10.1002/qj.2453, 2015.

842 Seigel, R. B. and van den Heever, S. C.: Dust Lofting and Ingestion by Supercell Storms, *J. Atmos. Sci.*, 69(5),
843 1453–1473, doi:10.1175/JAS-D-11-0222.1, 2012.

844 Sessions, W. R., Reid, J. S., Benedetti, A., Colarco, P. R., da Silva, A., Lu, S., Sekiyama, T., Tanaka, T. Y.,
845 Baldasano, J. M., Basart, S., Brooks, M. E., Eck, T. F., Iredell, M., Hansen, J. A., Jorba, O. C., Juang, H.-
846 M. H., Lynch, P., Morcrette, J.-J., Moorthi, S., Mulcahy, J., Pradhan, Y., Razinger, M., Sampson, C. B.,
847 Wang, J. and Westphal, D. L.: Development towards a global operational aerosol consensus: basic
848 climatological characteristics of the International Cooperative for Aerosol Prediction Multi-Model
849 Ensemble (ICAP-MME), *Atmos. Chem. Phys.*, 15(1), 335–362, doi:10.5194/acp-15-335-2015, 2015.

850 Shwehdi, M. H.: Thunderstorm distribution and frequency in Saudi Arabia, *J. Geophys. Eng.*, 2(3), 252–267,
851 doi:10.1088/1742-2132/2/3/009, 2005.

852 Skamarock, W. C., Klemp, J. B., Dudhia, J. O. G. D., and Barker, D. M.: A description of the Advanced Research
853 WRF version 3, NCAR Tech. Note NCAR/TN-4751STR, NCAR, <http://dx.doi.org/10.5065/D68S4MVH>,
854 Boulder, CO, 2008.

855 Slingo, A., Ackerman, T. P., Allan, R. P., Kassianov, E. I., McFarlane, S. A., Robinson, G. J., Barnard, J. C., Miller,
856 M. A., Harries, J. E., Russell, J. E. and Dewitte, S.: Observations of the impact of a major Saharan dust
857 storm on the atmospheric radiation balance, *Geophys. Res. Lett.*, 33(24), doi:10.1029/2006GL027869,
858 2006.

859 Sokolik, I. N. and Toon, O. B.: Direct radiative forcing by anthropogenic airborne mineral aerosols, *Nature*,
860 381(6584), 681–683, doi:10.1038/381681a0, 1996.

861 Stafoggia, M., Zauli-Sajani, S., Pey, J., Samoli, E., Alessandrini, E., Basagaña, X., Cernigliaro, A., Chiusolo, M.,

862 Demaria, M., Díaz, J., Faustini, A., Katsouyanni, K., Kelessis, A. G., Linares, C., Marchesi, S., Medina, S.,
863 Pandolfi, P., Pérez, N., Querol, X., Randi, G., Ranzi, A., Tobias, A., Forastiere, F. and null null: Desert
864 Dust Outbreaks in Southern Europe: Contribution to Daily PM₁₀ Concentrations and Short-Term
865 Associations with Mortality and Hospital Admissions, *Environ. Health Perspect.*, 124(4), 413–419,
866 doi:10.1289/ehp.1409164, 2016.

867 [Stephens, G. L., L'Ecuyer, T., Forbes, R., Gettelmen, A., Golaz, J.-C., Bodas-Salcedo, A., Suzuki, K., Gabriel, P.,](#)
868 [and Haynes, J.: Dreary state of precipitation in global models, *J. Geophys. Res.*, 115, D24211,](#)
869 [doi:10.1029/2010JD014532, 2010.](#)

870 [Sun, Y., Solomon, S., Dai, A., and Portmann, R. W.: How often does it rain? *J. Clim.*, 19, 916–934,](#)
871 [doi:10.1175/JCLI3672.1, 2006.](#)

872 Takemi, T.: Importance of the Numerical Representation of Shallow and Deep Convection for Simulations of
873 Dust Transport over a Desert Region, *Adv. Meteorol.*, vol. 2012, 1-13, doi: 10.1155/2012/413584, 2012.

874 Tanaka, T. Y. and Chiba, M.: A numerical study of the contributions of dust source regions to the global dust
875 budget, *Glob. Planet. Change*, 52(1–4), 88–104, doi:10.1016/J.GLOPLACHA.2006.02.002, 2006.

876 Tegen, I. and Lacis, A. A.: Modeling of particle size distribution and its influence on the radiative properties of
877 mineral dust aerosol, *J. Geophys. Res. Atmos.*, 101(D14), 19237–19244, doi:10.1029/95JD03610, 1996.

878 Teixeira, J. C., Carvalho, A. C., Tuccella, P., Curci, G. and Rocha, A.: WRF-chem sensitivity to vertical resolution
879 during a saharan dust event, *Phys. Chem. Earth, Parts A/B/C*, 94, 188–195,
880 doi:10.1016/J.PCE.2015.04.002, 2016.

881 Todd, M. C., Bou Karam, D., Cavazos, C., Bouet, C., Heinold, B., Baldasano, J. M., Cautenet, G., Koren, I., Perez,
882 C., Solmon, F., Tegen, I., Tulet, P., Washington, R. and Zakey, A.: Quantifying uncertainty in estimates of
883 mineral dust flux: An intercomparison of model performance over the Bodélé Depression, northern Chad, *J.*
884 *Geophys. Res. Atmos.*, 113(D24), doi:10.1029/2008JD010476, 2008.

885 Tulet, P., Crahan-Kaku, K., Leriche, M., Aouizerats, B. and Crumeyrolle, S.: Mixing of dust aerosols into a
886 mesoscale convective system: Generation, filtering and possible feedbacks on ice anvils, *Atmos. Res.*,
887 96(2–3), 302–314, doi:10.1016/J.ATMOSRES.2009.09.011, 2010.

888 Twohy, C. H., Kreidenweis, S. M., Eidhammer, T., Browell, E. V., Heymsfield, A. J., Bansemer, A. R., Anderson, B.
889 E., Chen, G., Ismail, S., DeMott, P. J. and Van Den Heever, S. C.: Saharan dust particles nucleate droplets
890 in eastern Atlantic clouds, *Geophys. Res. Lett.*, 36(1), doi:10.1029/2008GL035846, 2009.

891 Uno, I., Wang, Z., Chiba, M., Chun, Y. S., Gong, S. L., Hara, Y., Jung, E., Lee, S.-S., Liu, M., Mikami, M., Music,
892 S., Nickovic, S., Satake, S., Shao, Y., Song, Z., Sugimoto, N., Tanaka, T. and Westphal, D. L.: Dust model
893 intercomparison (DMIP) study over Asia: Overview, *J. Geophys. Res. Atmos.*, 111(D12),
894 doi:10.1029/2005JD006575, 2006.

895 van Donkelaar, A., Martin, R. V, Brauer, M., Kahn, R., Levy, R., Verduzco, C. and Villeneuve, P. J.: Global
896 estimates of ambient fine particulate matter concentrations from satellite-based aerosol optical depth:
897 development and application, *Environ. Health Perspect.*, 118(6), 847–855, doi:10.1289/ehp.0901623, 2010.

898 Woodage, M. J. and Woodward, S.: U.K. HiGEM: Impacts of Desert Dust Radiative Forcing in a High-Resolution

899 Atmospheric GCM, *J. Clim.*, 27(15), 5907–5928, doi:10.1175/JCLI-D-13-00556.1, 2014.

900 Yang, Q., Easter, R. C., Campuzano-Jost, P., Jimenez, J. L., Fast, J. D., Ghan, S. J., Wang, H., Berg, L. K., Barth,
901 M. C., Liu, Y., Shrivastava, M. B., Singh, B., Morrison, H., Fan, J., Ziegler, C. L., Bela, M., Apel, E.,
902 Diskin, G. S., Mikoviny, T. and Wisthaler, A.: Aerosol transport and wet scavenging in deep convective
903 clouds: A case study and model evaluation using a multiple passive tracer analysis approach, *J. Geophys.*
904 *Res. Atmos.*, 120(16), 8448–8468, doi:10.1002/2015JD023647, 2015.

905 Yang, Z.-L., Niu, G.-Y., Mitchell, K. E., Chen, F., Ek, M. B., Barlage, M., Longuevergne, L., Manning, K., Niyogi,
906 D., Tewari, M. and Xia, Y.: The community Noah land surface model with multiparameterization options
907 (Noah-MP): 2. Evaluation over global river basins, *J. Geophys. Res. Atmos.*, 116(D12),
908 doi:10.1029/2010JD015140, 2011.

909 Yin, Y., Chen, Q., Jin, L., Chen, B., Zhu, S. and Zhang, X.: The effects of deep convection on the concentration and
910 size distribution of aerosol particles within the upper troposphere: A case study, *J. Geophys. Res. Atmos.*,
911 117(D22), doi:10.1029/2012JD017827, 2012.

912 Yu, Y., Notaro, M., Kalashnikova, O. V and Garay, M. J.: Climatology of summer Shamal wind in the Middle East,
913 *J. Geophys. Res. Atmos.*, 121(1), 289–305, doi:10.1002/2015JD024063, 2016.

914 Yuter, S. E. and Houze, R. A.: Three-Dimensional Kinematic and Microphysical Evolution of Florida
915 Cumulonimbus. Part II: Frequency Distributions of Vertical Velocity, Reflectivity, and Differential
916 Reflectivity, *Mon. Weather Rev.*, 123(7), 1941–1963, doi:10.1175/1520-
917 0493(1995)123<1941:TDKAME>2.0.CO;2, 1995.

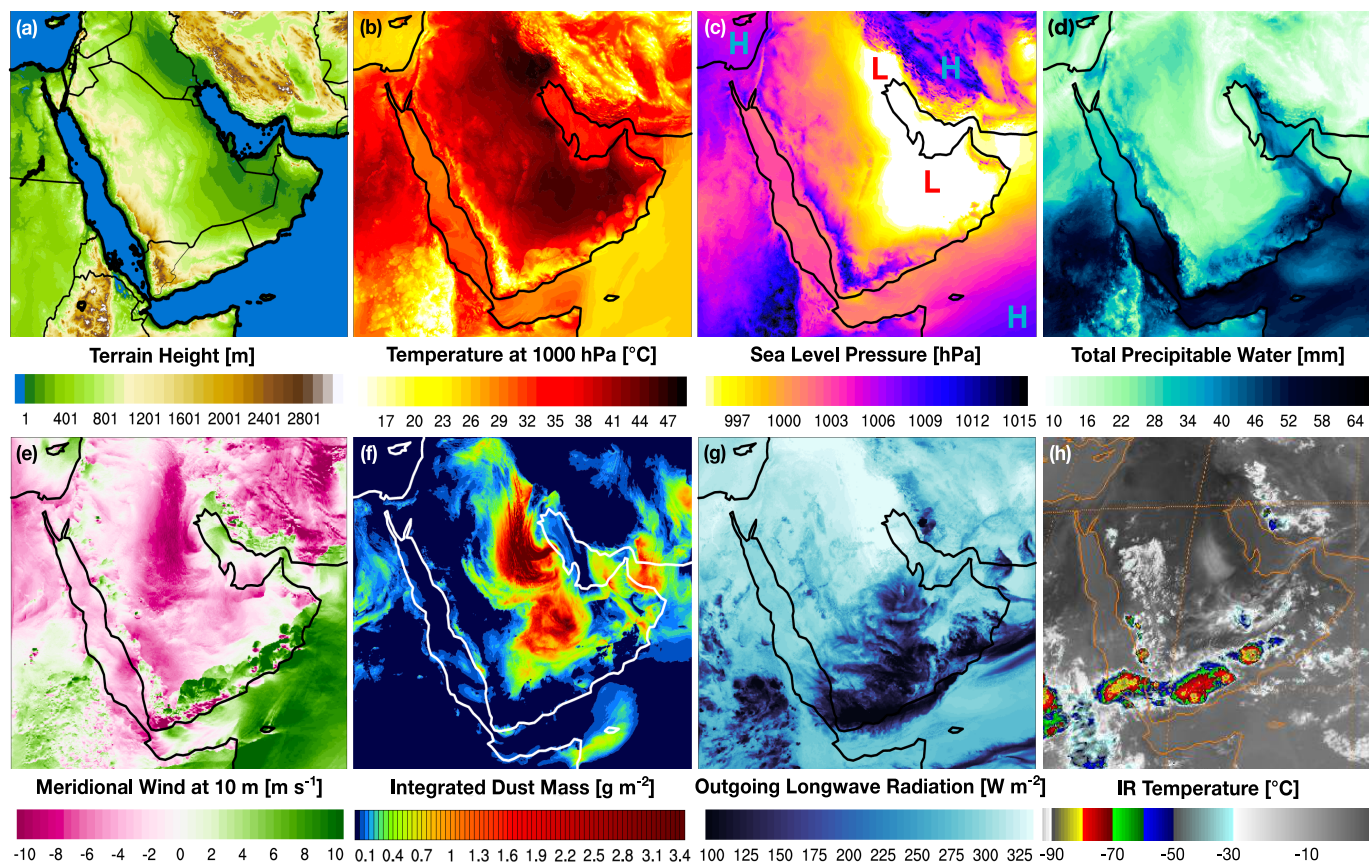
918 Zender, C. S., Miller, R. L. R. L. and Tegen, I.: Quantifying mineral dust mass budgets: Terminology, constraints,
919 and current estimates, *Eos, Trans. Am. Geophys. Union*, 85(48), 509–512, doi:10.1029/2004EO480002,
920 2004.

921 Zhao, C., Liu, X., Leung, L. R., Johnson, B., McFarlane, S. A., Gustafson Jr., W. I., Fast, J. D. and Easter, R.: The
922 spatial distribution of mineral dust and its shortwave radiative forcing over North Africa: modeling
923 sensitivities to dust emissions and aerosol size treatments, *Atmos. Chem. Phys.*, 10(18), 8821–8838,
924 doi:10.5194/acp-10-8821-2010, 2010.

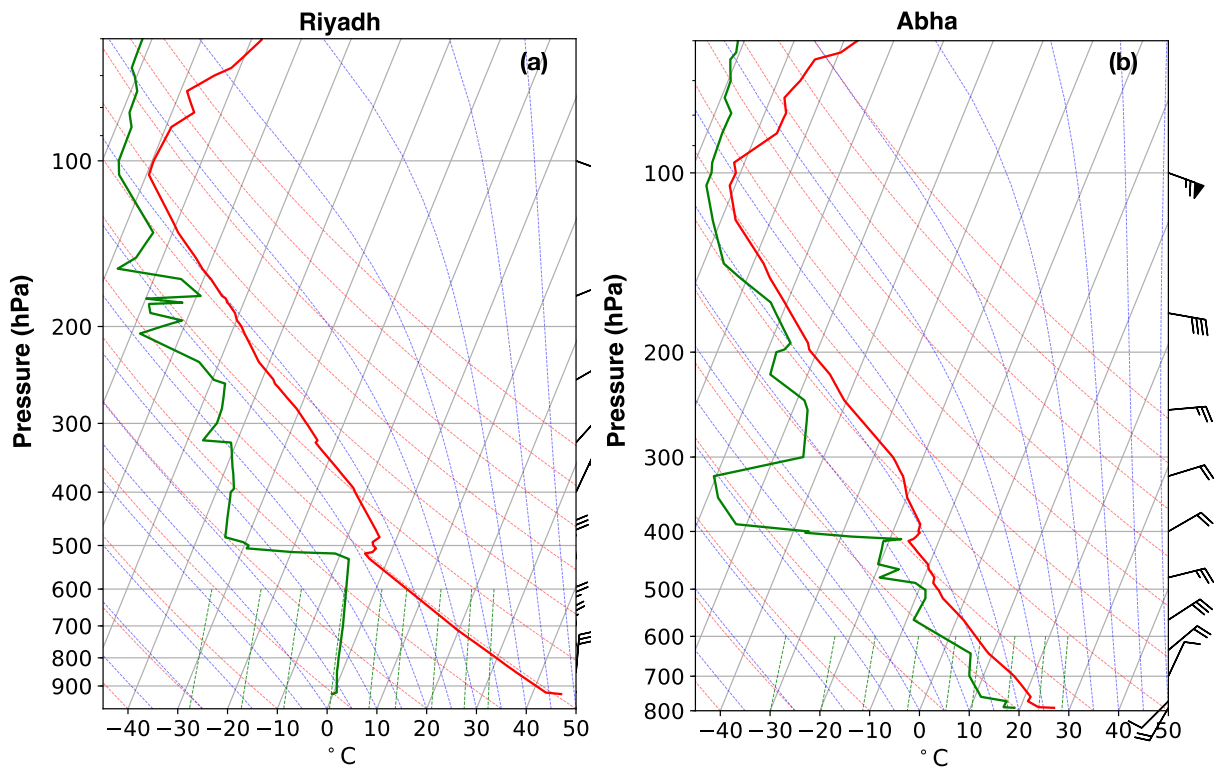
925

WRF-Chem Version 3.9.1.1	Parameterization / Model Option
Simulation Start	02-Aug-2016-00:00:00 UTC
Simulation End	05-Aug-2016-00:00:00 UTC
Domains	dx = dy = 45km / 15km / 3km
Nesting	One-way
Vertical Levels	50 stretched
Initialization	GDAS-FNL Reanalysis
Aerosol Module / Erodible Grid Map	GOCART / Ginoux et al. (2004)
Microphysics	Morrison 2-Moment
Radiation	RRTMG Longwave & Goddard Shortwave
Land Surface	Noah-MP Land Surface Model
Cumulus Schemes (45 km and 15 km grids only)	Betts–Miller–Janjic (BMJ) Kain–Fritsch (KF) Grell 3D Ensemble (GD) Tiedtke Scheme (TD) Simplified Arakawa–Schubert (AS)
Boundary Layer / Surface Layer	MYNN Level 3

926 **Table 1: Summary of WRF-Chem model options utilized and the simulation setup.**



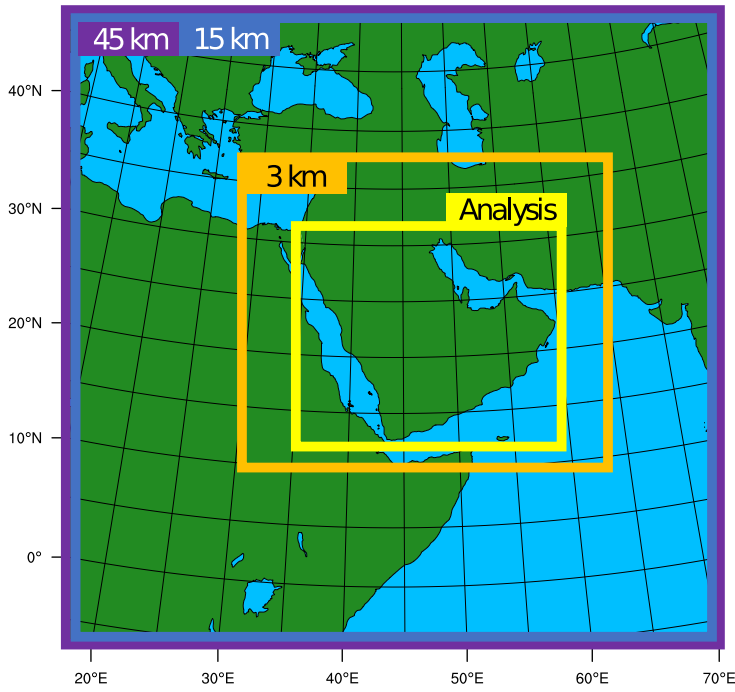
927
 928 **Figure 1: Case study topography and meteorology for August 3, 2016 at 15:00 UTC: (a) terrain height and national**
 929 **boundaries, (b) 1000 hPa Temperature, (c) sea level pressure, (d) total precipitable water, (e) meridional winds at 10 m**
 930 **AGL, (f) vertically integrated dust mass, (g) outgoing longwave radiation, and (h) IR temperature. Panel (h) is observed**
 931 **from Meteosat-7 while panels (a-g) are snapshots from the 3 km WRF-Chem simulation**



932

933 **Figure 2. Skew-T diagrams for two radiosonde release sites in Saudi Arabia on August 3, 2016 at 12:00 UTC for an inland**
 934 **location (a) and a location nearer to the coast (b).**

935



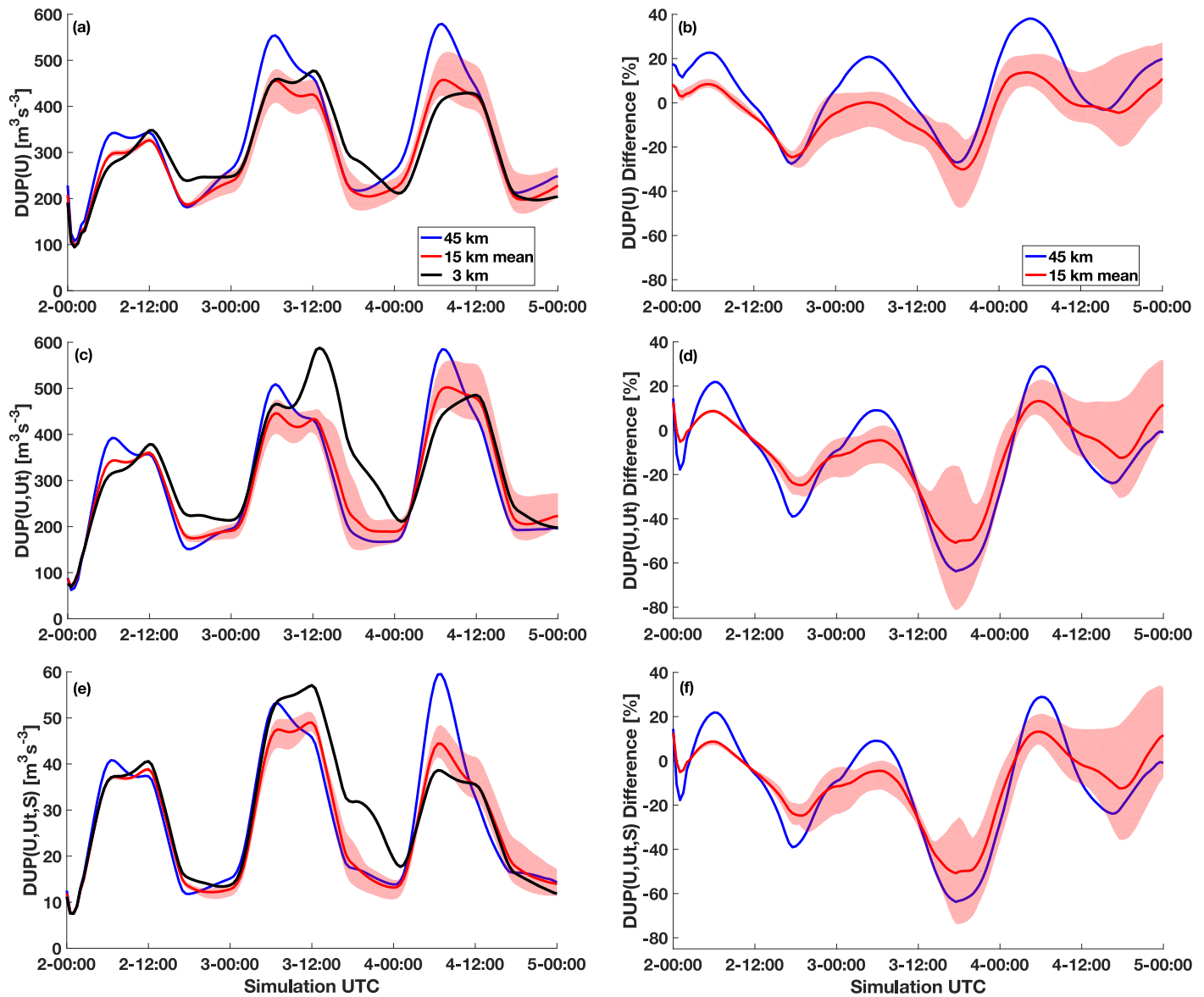
936

937

938

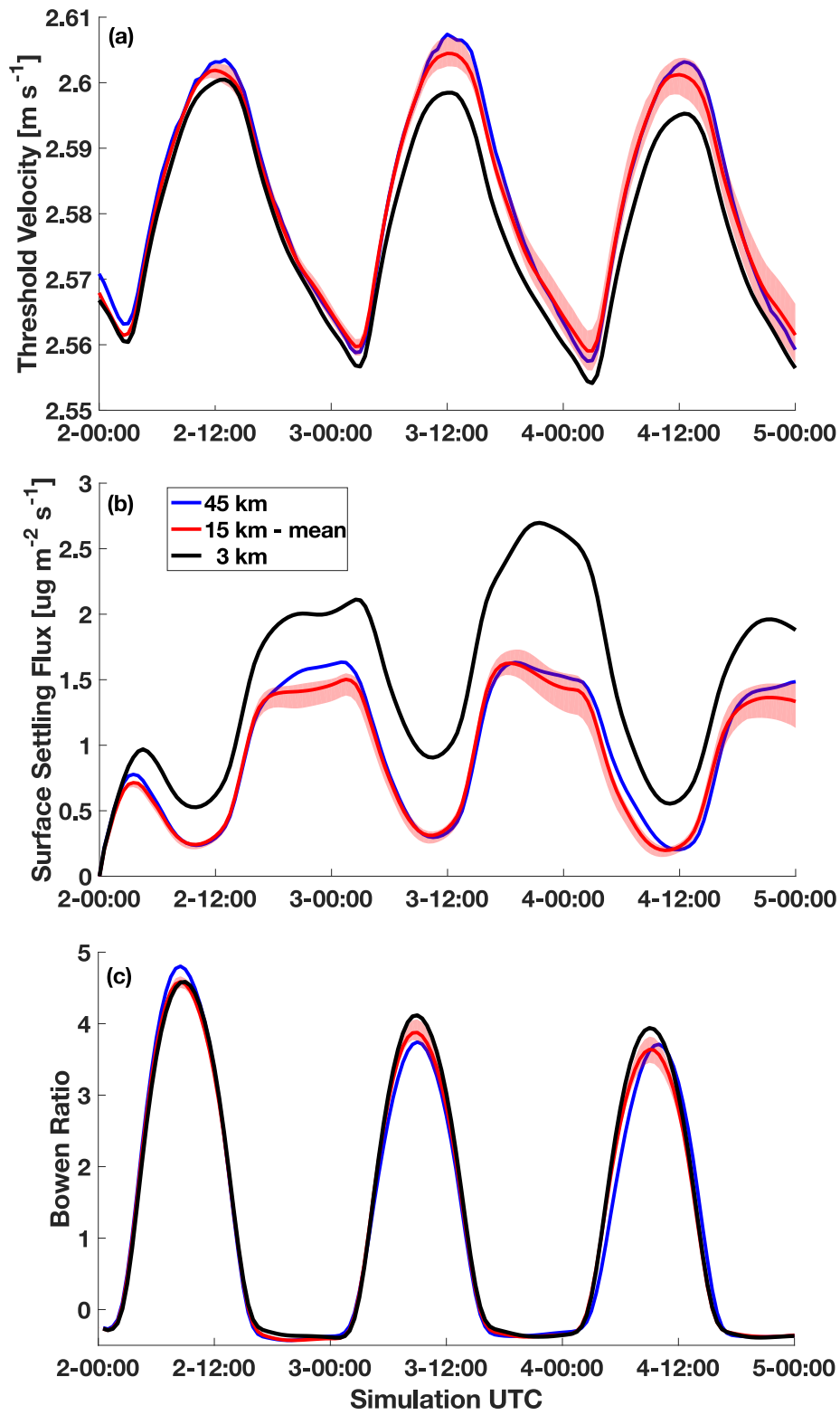
939

Figure 3: Model domain setup and analysis region for the 45 km (purple) and 15 km (blue) independent simulations with cumulus parameterizations, and the 3 km nested convection permitting simulation (orange). The averaging region for the analysis is denoted in yellow.



940

941 **Figure 4:** Left column: **domain-averaged** dust uplift potential for (a) DUP(U), (c) DUP(U, U_t), and (e) DUP(U, U_t, S)
 942 for the 45 km (blue), 15 km mean (red), and 3 km (black) simulations with the maximum and minimum spread across the
 943 15 km simulations indicated in light red shading. Note that in panel (e) there is a change in scale in the ordinate. Right
 944 column: percent difference between the 3 km convection-permitting simulation and the simulations employing cumulus
 945 parameterizations for the different DUP parameters.

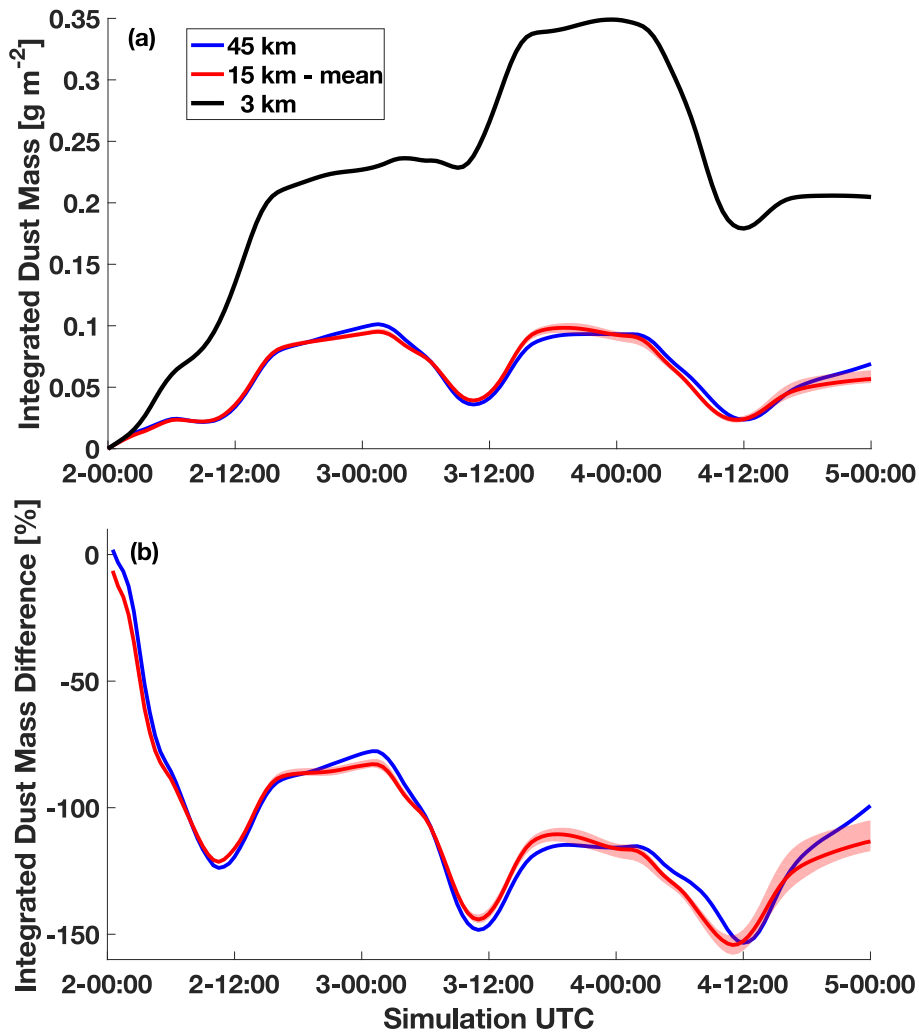


946

947

948

Figure 5: ~~Domain~~Spatially averaged (a) dust uplift threshold velocity, (b) dust surface settling flux, and (c) Bowen ratio of sensible to latent heat flux. Colors and shading are the same as in Fig. 4.

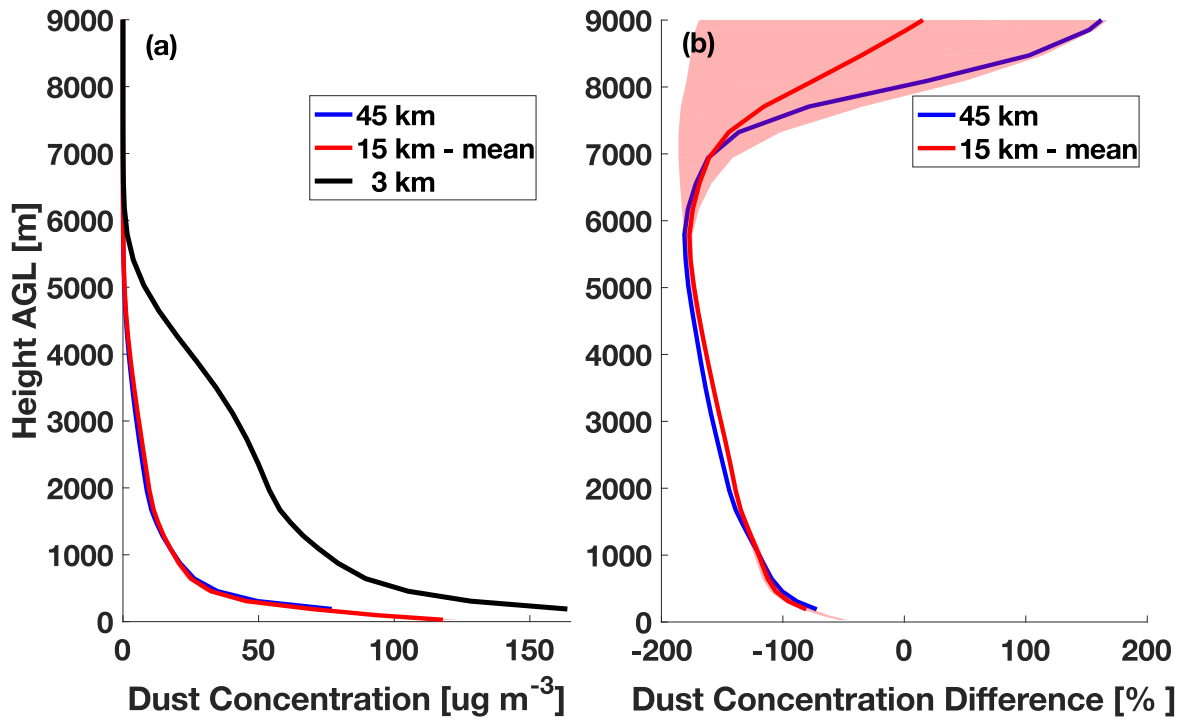


949

950

951

Figure 6: ~~Domain~~Spatially averaged, vertically integrated dust mass. Colors and shading are identical to that in previous figures.



952

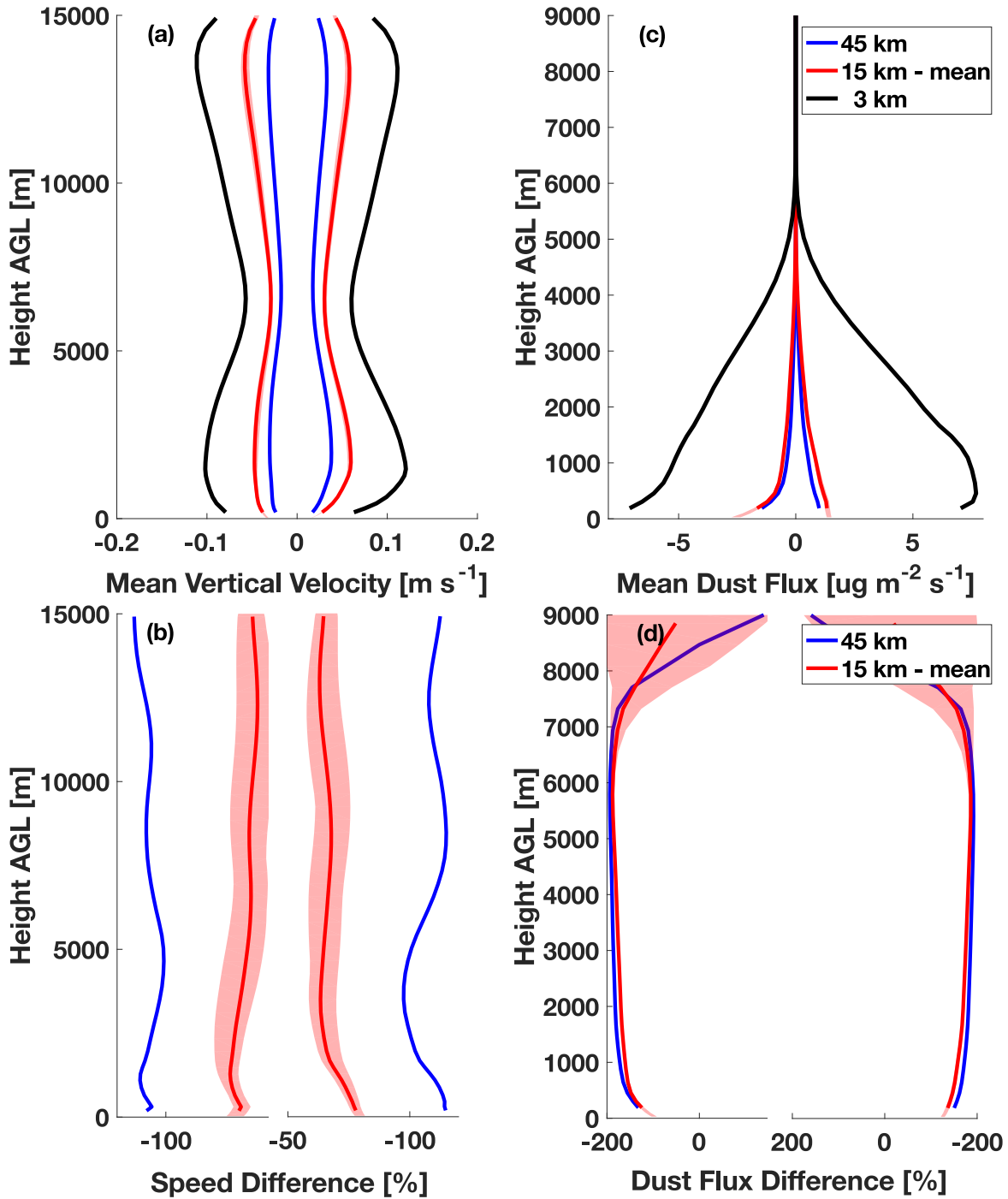
953

954

955

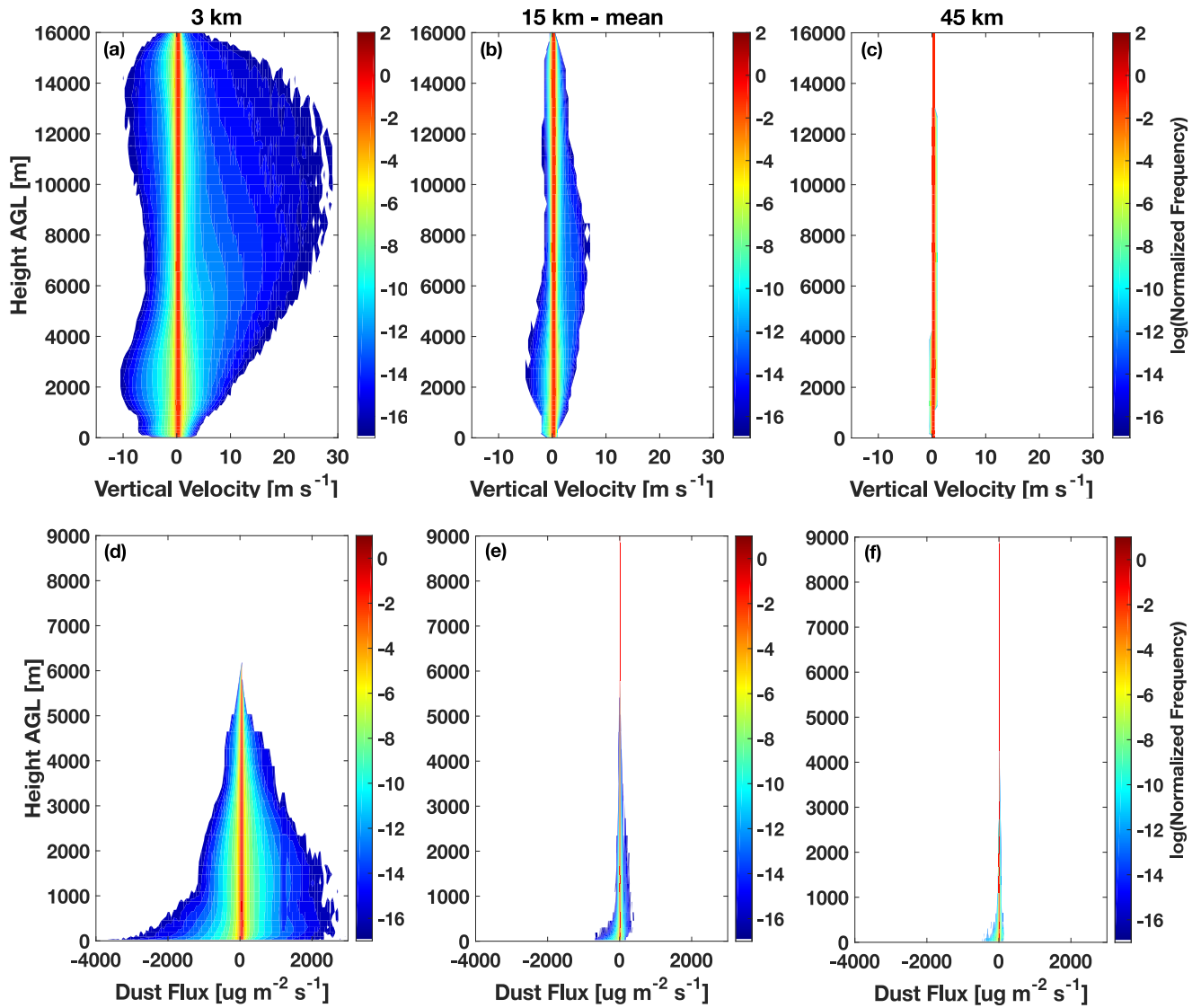
956

Figure 7: ~~Domain~~Spatially and time averaged vertical dust concentrations (a), with the (b) percent difference between the 3 km convection-permitting simulation and the simulations employing cumulus parameterizations. Plots are truncated at 9 km since the values above this height do not significantly vary from what is shown here. Colors and shading are identical to that in previous figures.



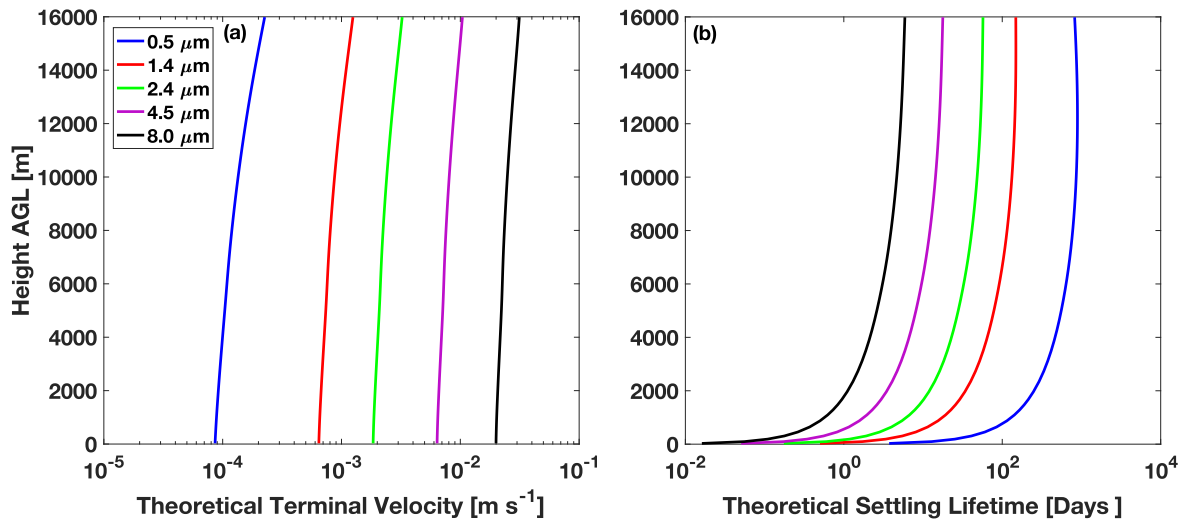
957

958 Figure 8. Left column: ~~domainspatially~~ and time averaged vertical velocities (a), with the (b) percent difference between
 959 the 3 km convection-permitting simulation and the simulations employing cumulus parameterizations. All velocities above
 960 or below zero were considered. Colors and shading are identical to that in previous figures. Right column: same but for
 961 vertical dust mass flux. Note that in panels (c) and (d) the vertical axes are truncated at 9 km since the values above this
 962 height do not significantly vary from what is shown here.



964

965 **Figure 9: Top row: Contoured Frequency by Altitude Diagrams (CFADs) for vertical velocity, normalized by the number**
 966 **of grid points in each respective simulation. The contours are computed on a log scale to highlight the variances away**
 967 **from zero. Bottom row: same but for vertical dust mass flux. Note that the panels in the bottom row are truncated at 9**
 968 **km since the values above this height do not significantly vary from what is shown here.**



969

970

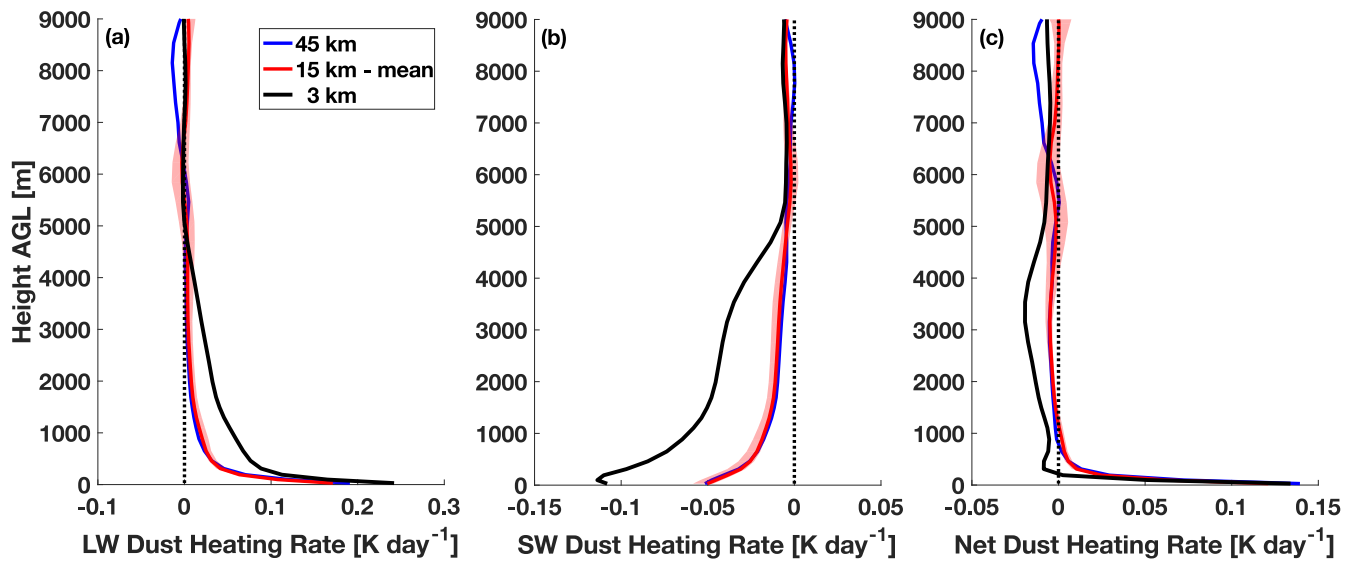
971

972

973

974

Figure 10: Theoretical terminal velocity of dust particles (a) based on Stokes settling velocity with slip correction for pressure dependence for the 5 effective radii of dust particles in WRF-Chem. The calculations assume no vertical motions, advection, deposition, coagulation, or condensation. (b) The lifetime of these theoretical dust particles based on their height in the atmosphere.



975

976

977

978

979

Figure 11: ~~Domain~~Spatially and time averaged longwave (a), shortwave (b), and net (c) dust heating rate profile for the 45 km (blue), 15 km mean (red), and 3 km (black) simulations with the maximum and minimum spread across the 15 km simulations indicated in light red shading. Plots are truncated at 9 km since the values above this height do not significantly vary from what is shown here.